

**MODELING AIRCRAFT FUEL CONSUMPTION
WITH A NEURAL NETWORK**

by
Glenn D. Schilling

Thesis submitted to the faculty of the
Virginia Polytechnic Institute and State University
in partial fulfillment of the requirements for the degree of

MASTER OF SCIENCE
IN
CIVIL ENGINEERING

APPROVED:

Antonio A. Trani, Ph.D., Chairman

Donald R. Drew, Ph.D.

Richard G. Greene, Ph.D.

February, 1997
Blacksburg, Virginia

Keywords: Aviation, Aircraft Performance, Backpropagation, Models

MODELING AIRCRAFT FUEL CONSUMPTION WITH A NEURAL NETWORK

by

Glenn D. Schilling

Dr. A. A. Trani, Chairman

Civil Engineering

(ABSTRACT)

This research involves the development of an aircraft fuel consumption model to simplify Bela Collins of the MITRE Corporation aircraft fuelburn model in terms of level of computation and level of capability. MATLAB and its accompanying Neural Network Toolbox, has been applied to data from the base model to predict fuel consumption. The approach to the base model and neural network is detailed in this paper. It derives from the basic concepts of energy balance. Multivariate curve fitting techniques used in conjunction with aircraft performance data derive the aircraft specific constants. Aircraft performance limits are represented by empirical relationships that also utilize aircraft specific constants. It is based on generally known assumptions and approximations for commercial jet operations. It will simulate fuel consumption by adaptation of a specific aircraft using constants that represent the relationship of lift-to-drag and thrust-to-fuel flow.

The neural network model invokes the output from MITRE's algorithm and provides: (1) a comparison to the polynomial fuelburn function in the fuelburn post-processor of the FAA Airport and Airspace Simulation Model (SIMMOD), (2) an established sensitivity of system performance for a range of variables that effect fuel consumption, (3) a comparison of post fuel burn (fuel consumption algorithms) techniques to new techniques, and (4) the development of a trained demo neural network.

With the powerful features of optimization, graphics, and hierarchical modeling, the MATLAB toolboxes proved to be effective in this modeling process.

ACKNOWLEDGMENTS

I sincerely wish to express my gratitude to my advisor Dr. Antonio Trani for his full support, expert guidance, understanding and encouragement throughout the course of this research. Also, I am greatly indebted to him for his critical review of the manuscript of my thesis.

I would like to thank my committee members, Dr. Donald Drew and Dr. Richard Greene, for serving on my committee, and providing me with excellent course instruction during my graduate years at Virginia Tech.

It is my greatest pleasure to dedicate this thesis to my parents, my dream was accomplished by their help. I would also like to thank my brother's and sister's-in-law for their unconditional support throughout my entire collegiate career.

Finally, I would like to thank the many friends who encouraged me to continue my higher education at Virginia Tech.

TABLE of CONTENTS

Chapter	Page
1. Introduction	
1.1 Purpose.....	1
1.2 Background.....	1
1.3 Fuel Consumption Modeling.....	2
1.4 Fuelburn Background.....	3
1.5 Research Approach, and Objective.....	5
2. Literature Review	
2.1 Introduction.....	7
2.2 Aerodynamic Forces.....	7
2.2.1 Temperature.....	9
2.2.2 Pressure.....	9
2.2.3 Density.....	10
2.2.4 Viscosity.....	12
2.2.5 Sonic Velocity.....	12
2.3 Performance Characteristics of Aircraft.....	15
2.4 Advanced Fuelburn Model Assumptions.....	17
2.5 Advanced Fuelburn Model (AFBM).....	18
2.6 The Power of Neural Networks.....	22
2.6.1 Elements of the Neural Network Paradigm.....	23
2.6.2 Network Architecture.....	26
2.6.3 Transfer Functions.....	27
2.6.4 Backpropagation.....	29
2.6.5 Levenberg-Marquardt Backpropagation Algorithm.....	31

Chapter	Page
3. Methodology	
3.1 Introduction.....	42
3.2 Models and Nonlinear Optimization.....	42
3.3 Approach to Model Development.....	44
3.4 Aircraft Fuel Consumption Model Assumptions	46
3.5 Description of MATLAB	47
3.6 Research Discussion and Pertaining Questions	48
4. Model Description	
4.1 Introduction.....	54
4.2 Specifics of the Neural Network.....	54
4.3 Statistics of Performance Data	60
4.3.1 Statistical Methods.....	60
4.4 Output of the Model.....	64
5. Model Application and Analysis	
5.1 Introduction.....	65
5.2 Model Application	65
5.3 Model Input Parameters	66
5.4 Model Results	69
5.4.1 Graphical Analysis.....	69
5.4.2 Statistical Analysis.....	79
5.5 Statistical Results	86
6. Conclusions and Recommendations	
6.1 Introduction.....	87
6.2 Conclusions.....	87
6.3 Recommendations.....	89
Bibliography	91

Appendix A. Aircraft Specific Constants	95
B. AFCM Program.....	100
C. MINITAB Session Worksheets	107
D. Weight and Bias Matrix Output of AFCM.....	110

LIST of FIGURES

Figure	Page
1. Flight Path Free Body Diagram.....	8
2. Layer of S Neurons with R Inputs.....	25
3. Two-Layer Tansig/Purelin Network	26
4. Tan-Sigmoid Transfer Function.....	28
5. BP Learning Schematics	30
6. Three-Layer Neural Network.....	51
7. Two Dimensional Input Vector.....	55
8. Partial Aircraft Echo Report.....	67
9. Velocity and Altitude Profiles.....	72
10. Fuel Consumption Before Network Training.....	73
11. Lift and Drag Relationships vs. Mach Number.....	74
12. Mach Functions vs. Mach Number	75
13. Trained vs. Actual Fuel Consumption and Generalized vs. Trained Fuel Consumption	76
14. Comparison of Fuel Consumption Data.....	77
15. Comparison of Specific Input Fuel Consumption Data	78
16. Summary of AFBM-NNOM Statistical Results.....	79
17. Fuel Consumption Differences of a Boeing 747-100.....	80
18. Fuel Consumption Differences of a Boeing 767-200.....	82
19. Fuel Consumption Differences of a Bombardier Dash-7.....	83
20. Fuel Consumption Differences of a McDonnell-DouglasDC10-30.....	84
21. Fuel Consumption Differences of a Lockheed Martin Jetstar.....	85
22. Summary of Statistical Results	86

LIST of TABLES

Table	Page
1. U.S. Standard Atmosphere.....	14
2. Floating Point Operations	68

1. INTRODUCTION

1.1 Purpose

The pace of advances in aeronautical technology from the Wright brothers to today's supersonic military and jumbo jets has been rapid and the demands intense. A need for increased speed, range, and payload are everpresent. In conjunction with these factors is fuel efficiency. Identifying the amount of fuel consumed by a given aircraft while moving in both airspace and ground networks is critical to air transport economics. Reducing the amount of fuel consumed involves knowing the effect of alternate profiles and procedures on fuel consumption or fuel flow for the various aircraft types operating in the system. Within the system a penalty in one area may be offset by benefits in other areas, hence, a net benefit in the system. The Federal Aviation Administration (FAA) and aviation community are striving to provide more fuel efficient operations in the system. Critical to many of the efforts is the ability to estimate fuel consumption. The MITRE Corporation, under FAA sponsorship, developed a fuel consumption algorithm designed to accept static constants relating to aircraft performance, and dynamic inputs describing the actual flight profile.

1.2 Background

At one time extraction costs and availability of aviation fuel had little impact on the evolution of the air transportation industry. Today, fuel conservation in aviation is one of the most critical concerns to air transportation companies. By the early 1970s it had become increasingly evident that the era of plentiful, inexpensive petroleum-based fuel was ending. The fuel cost was becoming more significant in air transport economics. In 1973 the price of commercial jet fuel was \$0.12 per gallon: during that year the Arab oil embargo spiked the market, and for the next two years the airlines faced a three-hundred

percent increase in jet fuel costs. In 1981 the price reached \$1.05. Six years later fuel prices declined reaching a low of \$0.53 per gallon. At the end of 1987, prices began to escalate following a similar trend to the previous years. In 1991 the price per gallon of commercial jet fuel was \$0.78. During the fiscal year 1994 FAA Aviation Forecasts determined jet fuel prices will generally decline, as stability returns to the jet fuel market. Fuel prices averaged \$0.55 in 1994. The forecast of jet fuel prices on the current dollars scale are expected to follow the trends of the previous years, indicating a four percent increase per year over 12 years. The technical report FAA Aviation Forecasts - Fiscal Years 1995-2006 reports that “the outlook for the 12-year period is moderate economic growth, stable real fuel prices, modest inflation, and continued moderate to strong growth in demand for aviation services.” Although the price per gallon of commercial aviation fuel has dropped since 1981, the number of enplanements (flights) increased annually. As the enplanements increase the demand and usage for jet fuel increases.

The commercial air transportation industry is faced with the challenge of maintaining a viable economic position in the face of aviation fuel costs in combination with increasing fuel consumption. Considering that more than (based upon mid-1990 commercial aircraft fuel consumption) twelve-billion gallons of fuel are burned each year by US commercial air transports, a one percent improvement in their operating efficiency would save 120 million gallons annually (Ethell, 1983). The motivation behind FAA’s efforts in fuel efficient operations research is the dramatic enhancement of the Air Transportation System. In order to achieve improved system efficiency a key requirement is an improved capability to accommodate fuel efficient aircraft operations. The close linkage between fuel usage and operator profitability necessitates the development and application of models that deliver energy performance of aircraft.

1.3 Fuel Consumption Modeling

SIMMOD-The FAA Airport and Airspace Simulation Model version 1.2 utilizes a fuelburn post-processor that defines and evaluates fuel efficient operations of an aircraft

flight profile. The fuelburn post-processor produces six individual reports determining the fuel consumed on the ground and in the airspace (SIMMOD, 1989a). The software utilizes the Advanced Fuel Burn Model - MOD 830725 (AFBM) developed by Bela P. Collins of the MITRE Corporation. The idea for this research stemmed from SIMMOD; looking for ways to make the software operate more efficiently incorporating a different approach in calculating fuel burn. The approach will be to eliminate the change in potential and kinetic energy equations along with several aircraft specific variables such as landing gear and flap settings from the AFBM, and design a point performance aircraft fuel consumption model (AFCM). The AFCM will incorporate the energy balance model and neural network model in order to simulate point fuelburn. This approach is described in full detail in Chapter 3 and 4.

The energy balance relation is defined as the aircraft travels along a path its energy gains and losses over a distance will be maintained. The fuelburn post-processor computes the fuel burning during every event of the simulation and fuel consumption of the aircraft. This model contains one-hundred seven aircraft profiles in its database ranging from GA (general aviation) to Heavy (wide body and jumbo jets). Currently the database accommodates nineteen of the one-hundred seven aircraft profiles, the rest of the fleet in the database utilizes the “best fit” constants and dynamic inputs relative to the aircraft assigned.

1.4 Fuelburn Background

Previously stated, the fuel consumption algorithm was designed to accept static constants associated with aircraft performance, and dynamic inputs describing the actual profile of the aircraft. Hence, fuel consumption can be estimated and expressed as

Energy Balance Approach (Collins, 1984)

$$(\text{energy change}) = (\text{energy in}) - (\text{energy loss})$$

or when expressed in terms of aircraft physical variables

$$f(E_T) - f(E_D) = f(\Delta KE) + f(\Delta PE),$$

where E_T is thrust energy, E_D is drag energy, and ΔKE and ΔPE are the changes in kinetic and potential energies respectively.

Using this approach the energy balance equation can estimate the thrust needed to overcome the aircraft drag within the path profile. Thrust can be written as

$$F_n = (\Delta KE + \Delta PE) / d + \underbrace{0.5\rho S_w V^2 (M_a + M_b C_L^2 + M_c C_L^4)}_{C_D},$$

where d is the distance of each flight segment, and C_D is the drag coefficient. Chapter 2 will contain a concise description for each of the above variables.

It is known that fuel consumption of a jet aircraft is a function of altitude, velocity and thrust. The energy balance and jet engine model equations are combined to formulate the fuel flow equation. However, the AFCM model uses an energy balance equation that does not include functions that compensate for aircraft configuration changes or estimating fuel consumption over an entire flight profile (ascent, cruise, descent). Therefore, the algorithm that will generate fuel flow for the AFCM can be written as the following empirical relationship

$$F_n = 0.5\rho S_w V^2 (M_a + M_b C_L^2 + M_c C_L^4),$$

where F_n is a point performance parameter.

The above equation does not express the change in potential and kinetic energy equations. The following equation is used to calculate point fuel flow and denoted as

$$W_f = F_1 + F_2F_n + F_3F_n^2,$$

where W_f is the fuel flow, F_1 - F_3 are fuel flow functions.

In order to satisfy the path profile concept the user would have to resolve two points in the AFCM to mimic a path profile and integrate over the area to find the change within the profile.

One note of caution at this juncture is that previous relationships should not be perceived as solutions to the very complex systems that exist in a turbojet engine. Instead Collins (1984) developed these functions to model the external engine performance without regard to what happens internally. Collins (1984) chose these functions because “they were well behaved”, “and the engine specific constants could be derived efficiently by multivariate regression” (Collins, 1984). These relationships proved to be accurate in modeling engine performance of seven different aircraft to within 4% maximum error.

1.5 Research Approach, and Objective

Based on the above discussion, modeling aircraft fuel consumption could prove to be an important factor in the Air Transportation Operations. The reason is simple, development of fuel consumption modeling establishes the performance of aircraft under specified conditions. Once these conditions are known then the process to find the most effective fuel flow rate can be determined. For example, by utilizing a fuel consumption model one can conclude that its best to fly a Boeing 747-100 at an altitude of 45,000 feet (FL450) traveling at Mach 0.86 rather than flying at FL445 traveling at Mach 0.84. This reasoning considers time as a factor, the actual fuel consumption per hour of the latter is less but the aircraft is traveling at a lower speed. Therefore, travel time is longer: the summation of fuel consumed is greater. Generally, it is believed that slower traveling vehicles consume less fuel. The previous example states otherwise, since aircraft

performance contains many more variables in determining fuel consumption it is hard to predict the behaviors that are highly nonlinear.

The objective of this research is to utilize a modeling simulation software to develop a flexible, computationally efficient, and accurate aircraft fuel consumption model. The model will consist of a reasonably straight forward neural network architecture; neural networks are somewhat similar to the polynomial approximation structure of the Advanced Fuel Burn Model - MOD 830725. Based on the assumption that Collins (1984) model depicts the most methodical and logical methods to date, his energy balance concept and a simpler neural net structure will prove to be an effective way to generate fuel consumption, and perhaps more efficient computationally.

A question asked during this research is whether a neural network can be less complex in terms of computational capability and yet deliver similar output to that of Collins algorithm. A comparison of the AFBM versus the Neural Network, the two levels of performance to compare are

- level of computation
- level of accuracy

This research presents the approach and methodology in building a computer model. MATLAB (Version 4.0, © Math Works, Inc., 1992) and accompanying Neural Network Toolbox (Version 2.0, © Math Works, Inc., 1994) has been applied to data from the base model (Collins, 1984) to predict fuel consumption. By channeling the information via neural net toolbox provides a means to conveniently simulate, graph, and model fuel consumption.

2. LITERATURE REVIEW

2.1 *Introduction*

The literature review is intended to present a background of the fundamentals of fuel consumption modeling with emphasis in techniques used to accurately establish aircraft fuel flow. Also, this review briefly describes aircraft performance characteristics which gives an understanding of how the air-side environment effects the vehicle. And how the neural network applications are utilized to model the fuel consumption.

2.2 *Aerodynamic Forces*

In order for an aircraft to achieve flight the basic equations of motion must be satisfied, where the lifting force and the weight of the vehicle are in equilibrium. The aircraft is assumed to be moving through still air over a flat non-rotating earth with its wings level (angle of attack, γ , approaching zero degrees) and with no side forces. Figure 1 represents the forces acting on an aircraft.

The motion of an aircraft in steady flight is determined by:

- its weight,
- the propulsive thrust exerted on the aircraft by the power plant,
- the aerodynamic force generated on the aircraft by its motion through the air.

Another important fact is that aircraft moves in a dynamic atmospheric environment which influences the performance of the vehicle. One normally thinks of altitude as the vertical distance of an aircraft above the earth's surface. However, the operation of an aircraft depends on the properties of the air through which it is flying, not

on the geometric height. Thus, the altitude is specified in terms of a standard atmosphere. When the air is assumed to be “standard” it means at sea level the atmosphere contains a known set of values for all of its properties. In retrospect, it almost never occurs in real life. At a given altitude, it’s sometimes hotter than it’s “supposed to be”, and sometimes cooler. Weather systems vary the atmospheric conditions, which makes a given elevation higher or lower than standard. Before analyzing the performance of aircraft it is important to thoroughly understand atmospheric behavior.

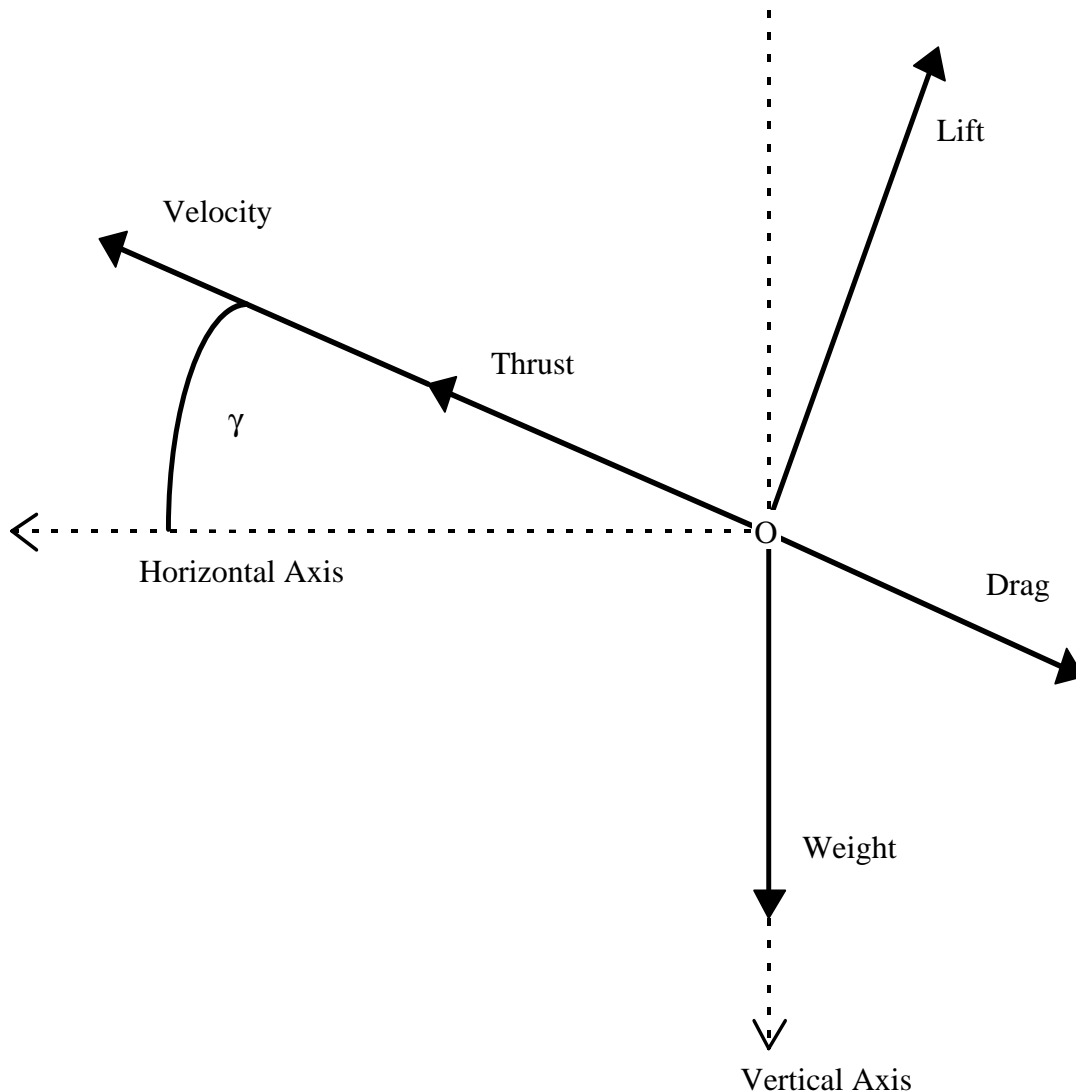


FIGURE 1: Flight Path Free Body Diagram (FBD).

Note: FBD components are described in section 2.3

For the air, the physical properties of interest are the temperature, pressure, density, viscosity and sonic velocity. Since atmospheric changes occur naturally and vary from day to day it is necessary to identify the conditions at all altitudes throughout the entire flight envelope. In 1962 a committee decided to establish the theoretical characteristics of a standardized atmosphere. The objective was to provide aircraft certification criteria throughout the world. A simplified version of the U.S. Standard Atmosphere, 1962 (Geopotential Altitude) is depicted in Table 1 and based on the following assumptions:

2.2.1 Temperature

At sea level, the standard temperature of the atmosphere is approximately 59.0°F (15.0°C). As the altitude increases the temperature decreases, initially at a constant rate, up to an altitude of approximately 36,000 feet (11 km). This area of temperature decline corresponds to the region of the atmosphere called the troposphere. An aircraft flying in this region experiences a temperature (linear) lapse rate of approximately 2.0°F per 1,000 feet. After breaching the troposphere (FL360) the next layer of atmosphere is called the stratosphere, and has a corresponding temperature of -69.7°F (-56.5°C). In the lower part of the stratosphere, the temperature remains nearly constant: a logarithmic variation which extends to an altitude of 75,500 feet (23 km). Since this area of research has an atmospheric upper boundary of 45,000 feet (13.7 km) there will not be any further interpolation of atmospheric characteristics past the lower part of the stratosphere.

2.2.2 Pressure

At sea level, the standard pressure of the air is 2,116.22 lb/ft² (1.01325x10⁵ N/m²). The pressure at any point in a stationary fluid is determined by the weight of the fluid above that point. When the altitude increases from sea level the pressure slowly decreases throughout both atmospheric regions. At the end of the troposphere the pressure is equal to only twenty-two percent of the pressure at sea level (USAF, 62). The rate of

change of pressure is associated with the rate of change of density; elaborating on both in the next section.

2.2.3 Density

At sea level, the standard density of the air is 0.0765 lb/ft³ (1.225 kg/m³). The air becomes less dense as altitude increases. To understand this relationship there are two basic equations governing density as a function of altitude. Where the air is treated as a gas, the first equation for the atmosphere with respect to density (ρ), temperature (T°), and pressure (p) is

$$p = \rho RT^\circ, \quad (2.1)$$

where R is the universal gas constant. The second equation states that the rate of change of pressure equals the weight of atmosphere, as the altitude changes. Hence, the equation is

$$\frac{dp}{dh} = -\rho g, \quad (2.2)$$

where g is the acceleration due to gravity. It is assumed that the gas (air) is at rest, all the forces acting on it must be in equilibrium. Hence, by summing the vertical forces results in the static pressure equation.

From the equation of state comes

$$\frac{d\rho}{\rho} = \frac{dp}{p} - \frac{dT^\circ}{T^\circ}, \quad (2.3)$$

which, combined with Eqs. (2.1) and (2.2), gives

$$\frac{dp}{\rho} = -\left(\frac{g}{RT^\circ} + \frac{1}{T^\circ} \frac{dT^\circ}{dh}\right)dh. \quad (2.4)$$

The previous equation can be written in the simpler form

$$\frac{d\rho}{\rho} = -\beta dh, \quad (2.5)$$

where β is the bracketed term in Eq. (2.4) and defined as the reciprocal of the scale altitude. Using this differential form for the density, the atmosphere can be represented as a locally exponential atmosphere. The coefficient β can be considered as constant over some small increment of altitude, then the integrated density function for the stratospheric condition is

$$\rho = \rho_0 e^{-\beta h}, \quad (2.6)$$

where ρ_0 is the density at the reference level and h is the altitude measured from this level. Previously stated, in the lower part of the stratosphere the temperature remains constant and therefore $\beta = g/RT^\circ$ remains constant if the variation of g with respect to altitude is neglected. In the troposphere, T° is a linear function of altitude, and β is a function of altitude. One author believes it is convenient to use the exponential atmosphere model given in Eq. (2.6) for both regions.

The atmospheric models used by Collins (1984) are closely correlated with the above relationships between the pressure and density. By substituting the dT°/dh for the constant temperature gradient into Eq. (2.5) and integrating from the condition at sea level, the troposphere model becomes

$$\rho = \rho_0 \left(1 + \frac{T^\circ}{T_0^\circ} h\right)^{-\frac{1}{T^\circ}(g/R+T^\circ)}. \quad (2.7)$$

This equation is termed the law of variation of density with respect to altitude in the troposphere according to the standard atmosphere. This research utilizes both atmospheric models, and is based on the assumption that density variation can be

calculated by the linear lapse rate model for altitudes less than or equal to 36,089 feet and the logarithmic variation model for altitudes greater than 36,089 feet (see Eqs. 2.12, 2.13).

2.2.4 Viscosity

When understanding viscosity, think of it in relation to the flow of a fluid. A highly viscous fluid has slow moving, thick and sticky characteristics. Where as low viscous fluids tend to be less glutinous, moving with ease. “Viscosity is in the form of tangential stress distributed within the fluid whenever there is relative motion. Hence a velocity gradient exists, in particular where the fluid moves over the surface of the vehicle. This is measured by the dynamic viscosity, μ , defined as the ratio of viscous stress to the velocity gradient” (McCormick, 1995). At sea level, the standard coefficient of viscosity of air is 1.2024×10^{-5} lb/ft-sec (1.7894×10^{-5} N-s/m²). The coefficient μ , depends only on its temperature, and decreases as the temperature decreases with altitude in the troposphere. It becomes constant in the stratosphere.

An explicit formula for computing the value of μ is

$$\frac{\mu}{\mu_0} = 0.081480723 \frac{T^{3/2}}{T+110.4} [\text{N-s/m}^2] . \quad (2.8)$$

The ratio of μ and the density of the air is named kinematic viscosity:

$$v = \frac{\mu}{\rho} \quad (2.9)$$

2.2.4 Sonic Velocity

“The speed of sound is the rate at which a small disturbance on the ambient condition travels through the air” (Ruijgrok, 1990). It can be shown that the speed of

sound is related to the lapse rate model and altitude. The speed decreases at a constant rate up to an altitude of approximately 36,000 feet (11 km), and then remains constant throughout the lower portion of the stratosphere. It can be found that the speed of sound, a , is equal to its initial condition a_0 minus the lapse rate (λ) times the altitude. The equation is shown below:

$$a = a_0 - \lambda(h), \quad (2.10)$$

where a_0 is the sonic velocity at sea level, and λ is

$$\lambda = \frac{661.5 - 573.6}{36089}. \quad (2.11)$$

Now that the basic understanding of atmospheric properties has been explained, the next step is to apply these concepts to predict aircraft performance.

TABLE 1: United States Standard Atmosphere, 1962

Altitude ft	Temperature °F	Temperature R	Pressure lb/ft ²	Density slugs/ft ³	Kinematic viscosity ft ² /s	Speed of sound ft/s
0	59.0	518.69	2116.2	2.3769E-03	1.5723E-04	661.5
5,000	41.2	500.86	1760.9	2.0482E-03	1.7755E-04	650.0
10,000	23.3	483.04	1455.6	1.7556E-03	2.0132E-04	638.3
15,000	5.5	465.23	1194.8	1.4962E-03	2.2927E-04	626.4
20,000	-12.3	447.43	937.26	1.2673E-03	2.6234E-04	614.3
25,000	-30.2	429.64	786.33	1.0663E-03	3.0168E-04	601.9
30,000	-48.0	411.86	629.66	8.9068E-04	3.4884E-04	589.3
35,000	-65.8	394.08	499.34	7.3820E-04	4.0575E-04	576.4
40,000	-69.7	389.99	393.12	5.8727E-04	5.0560E-04	573.6
45,000	-69.7	389.99	309.45	4.6227E-04	6.4223E-04	573.6
40,000	-69.7	389.99	393.12	5.8727E-04	5.0560E-04	573.6
45,000	-69.7	389.99	309.45	4.6227E-04	6.4223E-04	573.6

U.S.S.A , 1962 - Definition of Standard Atmosphere

A standard atmosphere is a hypothetical vertical distribution of atmospheric temperature, pressure, and density which by international or national agreement is taken to be representative of the atmosphere for the purpose of altimeter calibrations, aircraft design, performance calculations, etc. The internationally accepted standard atmosphere is called the International Civil Aeronautical Organization (ICAO) Standard Atmosphere or the International Standard Atmosphere (ISA). The U.S. Standard Atmosphere, 1962 is in agreement with the ICAO Standard Atmosphere up to 65,000 feet altitude. It is ideal air devoid of moisture, water, vapor, and dust, and obeys the perfect gas law. It is based upon accepted standard values of sea level air density, temperature and pressure.

2.3 Performance Characteristics of Aircraft

The ideal aircraft would be economical to buy, maintain, have a large seating capacity, and be fuel efficient. It's highly unlikely for an aircraft to have all of these characteristics but it is possible to retain a few. The goal in aircraft design is to achieve a rational balance between vehicle performance in combination with affordability.

To determine aircraft performance during level flight at any point in the flight path the following Aircraft Fuelburn Model (AFBM) can be utilized. This model uses the energy balance concept minus the changes in kinetic and potential energies. The energy balance equation, as previously described in the introduction, is written as

$$E_T = \Pi E_D,$$

where the thrust energy, E_T equals the product of the drag energy, ΠE_D .

The energy balance equation now becomes

$$F_n = DC_D$$

where thrust (F_n) equals the Drag (D) multiplied by the Drag Coefficient (C_D). Further explanation of this concept is Section 2.5.

It is important to describe the path profile equations so that the reader can see the difference of path and point performance. Each of the functional relationships expressed as energy terms can be related to the aircraft performance and **path** profile variables as follows:

$$\Delta KE = f(V_1, V_2, W_1, W_2),$$

$$\Delta PE = f(h_1, h_2, W_1, W_2),$$

$$E_D = f(\rho, V, S_w, C_D, X),$$

$$X = f(V, T),$$

where

- V_1 and V_2 are the incremental initial and final true airspeeds (TAS) expressed in ft/sec.
- W_1 , and W_2 are the incremental aircraft weight expressed in lb.
- h_1 , and h_2 are the incremental initial and final density altitudes expressed in feet.
- ρ is the incremental density of the atmosphere expressed in lb-sec²/ft.
- T is incremental travel time expressed in sec.
- X is incremental distance expressed in feet.

In the previous relationships, all of the variables are known path profile dependent except the wing area (S_w [ft²]) and drag coefficient (C_D). The wing area (S_w) is known for each individual aircraft but C_D has a unique relationship with the lift coefficient (C_L). Hence, C_L must be obtained under specific operating conditions that provide the required lift; then C_D can be determined.

The corresponding kinematic equations governing the aircraft motion in the vertical plane are

$$m \dot{V} = T - D - W(\sin\gamma),$$

$$m \dot{V} \gamma = L - W(\cos\gamma),$$

$$\dot{X} = V(\cos\gamma),$$

$$\dot{h} = V(\sin\gamma),$$

where X is the range, h is the altitude, V is the true airspeed, T is the thrust, D is the drag, L is the lift, W is the aircraft weight, m is the aircraft mass, and γ is the flight angle.

The motion of an aircraft can be represented by a quasi-steady-state condition where the velocity (TAS) and altitude change very slowly so that their respective time derivatives are assumed to be approximately zero (Roskam, 1989b). With these assumptions, the four equations above reduce to lift-equals-weight and thrust-equals-drag.

2.4 Advance Fuelburn Model (AFBM) Assumptions

An aircraft path profile can be described by considering the changes in velocity or true airspeed (V), altitude (h), and time (T). In order to derive the simplest form of the energy balance equation, the total path profile is divided into increments of approximately 2,000 ft altitude changes in the case of climbs and descents, or approximately 200 seconds during level flight. It has been found that this size increment yields the level of accuracy desired, when using both actual and performance handbook data. Other increments can be chosen, based upon accuracy requirements of a particular application. Additionally, use of increments permits the following simplifying assumptions:

1. An average atmospheric density (ρ) is used for calculations over the increment.
2. The aircraft weight change over an increment is small as compared to the total weight, therefore an average weight (W) is used for incremental calculations.
3. The acceleration during an increment is constant (a).
4. The flight path angle (γ) is small, therefore $\cos\gamma \cong 1$, or the aircraft weight equals the required lift.
5. Climb and descent rates are linear in an increment, thus $h_2 = h_1 + GX$.
6. Upper wind effects on fuel consumption are not a part of the computational requirement; therefore the velocity [TAS] equals the ground speed.
7. The functional forms used for lift vs. drag, and thrust over fuel flow, are sufficient to obtain a good data fit over the desired speed range.
8. The standard US atmospheric conditions apply, thereby permitting the density variation with altitude to be calculated by using the following equations:

$$\rho = 0.0023769 (1 - 0.00000688 * h)^{4.2563} \quad (2.12)$$

for altitudes equal to or less than 36,089 ft, and

$$\rho = 0.0007062 \exp\left[\frac{36,089 - h}{20,806.5}\right] \quad (2.13)$$

for altitudes greater than 36,089 ft.

2.5 Advanced Fuelburn Model

The fuelburn of an aircraft basically depends on airframe drag, engine specific fuel consumption, distance of the route to be flown, vertical flight path and aircraft weight. The central factor in every aspect of engine development, is to drive down thrust specific fuel consumption (TSFC), or simply called the specific fuel consumption (SFC). SFC is a measure of engine efficiency, defined as fuel flow rate in pounds per hour divided by engine thrust in pounds of force (lb/hr/lb). Hence, the lower the ratio the lower the fuel flow rate for a given thrust the lower the fuel consumption and more efficient the engine. The amount of fuel burned by an aircraft is highly variable with respect to the power plant, in this case (as to the research) its function is of two factors, altitude and velocity.

To find the energy consumption relations of an aircraft, the energy balance equation is appropriate and easily understood. It's expressed as a function of known variables that are either aircraft-type performance parameters, or path profile variables (Collins, 1980a). In order to calculate the estimated fuel consumption a relationship is needed between fuel burn and thrust. The fuelburn model uses this relationship incorporating the previous functional relationships (Section 2.3) with engine fuel flow rates. In Chapter 1, Section 1.4 the fuel flow equation represents a series of coefficients and variables. This section will describe the steps leading up to this equation allowing for a full understanding of the fuelburn model.

From the generalized relationship the change in kinetic and potential energy will not be included. Since this is a steady state analysis the terms go to zero. Using this approach the energy balance equation will now be a point performance equation that can

estimate the thrust needed to overcome the aircraft drag at any specified point within a level profile. Thrust can be written as

$$F_n = 0.5 * \rho * S_w * V^2 * (M_a + M_b * C_L^2 + M_c * C_L^4) . \quad (2.14)$$

Since the lift is equal to the weight it can be expressed as

$$L = W = 0.5 \rho S_w V^2 C_L, \quad (2.15)$$

solving for C_L :

$$C_L = W / 0.5 \rho S_w V^2, \quad (2.16)$$

the drag is also expressed as

$$D = 0.5 \rho S_w V^2 C_D . \quad (2.17)$$

Functionally the drag coefficient can be written in terms of the lift coefficient as

$$C_D = f(C_L, M),$$

where the Mach number (M) is considered to be the average Mach number.

At this juncture in time we will no longer associate the AFBM as a path performance model, and will now be interpreted as a point performance model.

In “Aviation Fuel Consumption Symposium”, Collins *et al.*, 1984, notes that a great deal of the performance data concerning both an airframe and an engine represents an approximation of how a typical air vehicle will function. These approximations represent a blending of theoretical, wind tunnel, and actual flight test results. Therefore

the accuracy of the fuel burn model is largely determined by the ingenuity and effort that is exercised in determining the appropriate mathematical functions based on the performance data. Then these functions are calibrated and verified by utilizing actual flight test data.

The conception of the fuel consumption model was determined by data sets consisting of approximately six-hundred data points (for various altitudes, mach numbers and throttle settings) to derive the equations for each aircraft model. Collins reports that this implicit model achieves a standard deviation of 1.4% from engine specifications of the actual consumption's observed in the field. And an upper limit of 4% difference between actual and predicted results has been imposed in the derivation of these multi-variant equations.

For estimation purposes, the total drag coefficient of a trimmed rigid aircraft can be expressed as

$$C_D = \left[\left(\sum C_{D_{P_{min}}} \right) + (C_{D_t}) + (C_{D_{int}}) + (C_{D_r}) + (C_{D_i}) + (C_{D_{PC_L}}) + (C_{D_c}) \right],$$

where

- $\sum C_{D_{P_{min}}}$ = Summation of the minimum profile drag of the individual aircraft components, for smooth turbulent attached flow.
- C_{D_t} = Drag required to trim the aircraft about its center of gravity.
- $C_{D_{int}}$ = Drag due to interference between components.
- C_{D_r} = Drag due to surface distributed roughness, steps, gaps, and significant protuberances.
- C_{D_i} = Wing vortex induced drag at a given wing lift coefficient corresponding to the spanwise distribution of lift, and is the net effect of elliptic and non-elliptic contributions.
- $C_{D_{PC_L}}$ = Net aircraft lift-dependent profile drag, including major contributions from the wing and fuselage, and other components.
- C_{D_c} = Compressibility Drag; this includes subcritical drag creep, wave drag, and shock-induced separation drag.

The first four terms are not lift dependent, the remaining terms are both lift and Mach dependent. Collins (1980b) also states that the following functions can be utilized to present the nondimensional drag coefficient (C_D) that consists of a nonlinear drag polar with sensitivity to Mach number:

$$C_D = M_a + M_b C_L^2 + M_c C_L^4, \quad (2.18)$$

where M_a , M_b , and M_c are functions of Mach number representing the first four terms, the fifth and sixth term, and the last term respectfully.

The three aircraft drag coefficient functions are defined as

$$M_a = K_1 + K_2 \Gamma^2 + K_3 \Gamma^4, \quad (2.19)$$

$$M_b = K_4 + K_5 \Gamma + K_6 \Gamma^2 + K_7 \Gamma^3 + K_8 \Gamma^4, \quad (2.20)$$

$$M_c = K_9 + K_{10} \Gamma + K_{11} \Gamma^2 + K_{12} \Gamma^3, \quad (2.21)$$

where K_n is the aircraft specific drag coefficient constant, and Γ is the Mach number ratio. In Chapter 5, Figure 12 represents plots of M_a , M_b , and M_c vs. Mach number to illustrate how the influence of drag varies relative to speed.

The model consists of aircraft specific constants and aircraft variables. To compute the fuel flow over a selected altitude and velocity a technique must be used to translate thrust into fuel flow. As stated in the introduction the fuel flow (W_f) is represented by the following empirical relationship:

$$W_f = F_1 + F_2 F_n + F_3 F_n^2, \quad (2.22)$$

where F_1 , F_2 , and F_3 are aircraft fuel flow functions, and expressed as

$$F_1 = C_1 + C_2 M + C_3 h + C_4 Mh + C_5 h^2 + C_6 Mh^2, \quad (2.23)$$

$$F_2 = [C_7 + C_8 M + C_9 h + C_{10} Mh + C_{11} h^2 + C_{12} Mh^2](N \cdot 10^4)^{-1}, \quad (2.24)$$

$$F_3 = [C_{13} + C_{14}M + C_{15}h + C_{16}Mh + C_{17}h^2 + C_{18}Mh^2](N \cdot 10^4)^{-2} . \quad (2.25)$$

With the exception of the change in dynamic and kinematic energies, and configuration changes of the aircraft (landing gear and flap extension) Collins (1984) fuel burn model utilizes the above core equation to compute the fuel burn. In this case the current model, AFBM (steady state) might be considered not as sensitive as the original but a simplified model that utilizes neural network technology. This concept is supposed to induce further research in the field of aviation fuel consumption via neural networks, and act as the foundation to more intricate fuel flow studies. Therefore, the object of this research is to utilize a modeling simulation software in combination with a neural network to develop a flexible, computationally efficient, and accurate fuel consumption model that can utilize any aircraft specifics.

2.6 The Power of Neural Networks

Neural networks, or simply neural nets, are computing systems which can be trained to learn a complex relationship between two or many variables or data sets. Basically, they are parallel computing systems composed of interconnecting simple processing nodes (Lau, 1992). Neural net techniques have been successfully applied in various fields such as function approximation, control systems and signal processing. Some examples that directly apply to transportation are truck brake diagnosis systems, vehicle scheduling, and routing systems. In the present application where a certain relationship exists between a data set of a particular aircraft point profile and its generalization on all possible data set pairs, neural nets can be used to efficiently predict the fuel consumption, given velocity and altitude of the vehicle. The data set needed for the neural net can be an actual steady state flight profile previously recorded or a generic one provided by an analytical model.

Neural networks utilize a matrix programming environment making most nets mathematically challenging. It should be understood that it is only the intent here to give

the reader a brief synopsis of neural networks, and describe the basic type of neural network used for the research. For a more in-depth review of the intensive mathematical derivation and computation of the neural networks please refer to the listed references mentioned throughout this section.

2.6.1 Elements of the Neural Network Paradigm (Hagan *et al.* 1996)

The neuron model and the architecture of a neural network describe how a network transforms its input into output. This transformation can be viewed as a computation. The model and the architecture each place limitations on what a particular neural net can compute. The way a network computes its output must be understood before training methods for the net can be explained.

Each neuron is represented by a vector of weights, a scalar (single real number), and a bias, and the neuron's transfer function. The products of the neuron's inputs and weights are summed with the neuron's bias and passed through the transfer function to get the neuron's output. Keep in mind this is an implicit description of how a neural network calculates.

A vector is a useful way to describe a pattern of numbers. For example the pattern of numbers that describe altitude and velocity (input vectors) and the fuel consumption (target vector) of an aircraft. Suppose that an aircraft (Boeing 747-100) is at FL360, and traveling at a true airspeed (TAS) of 280 knots consuming 36,000 pounds of fuel per hour. This information can be summarized in a vector or ordered list of numbers. In fact, a vector can have many parameters accompanying multidimensional space creating a very powerful and influential neural network. The neural net recognizes the input vectors as a set of weights on the input lines connected to a feedforward enhanced backpropagation (BP) processing unit (BP is classified as a neural net learning rule, and will be explained in a further section) that delivers the weighted outcome or target vector, a .

Neurons may be simulated with or without biases. A bias is much like a weight, except that it has a constant input of 1. The constant biases are used to adjust the fuel consumption model data (input parameters) into a form that the neural net can handle

easy. The purpose of the addition bias is to reduce the relative spread of the data for each net input, n . For example if the sets of input/output range considerably, an addition bias can be added to all the output to reduce the spread. Decreasing the spread in the data reduces the training time of the neural net.

The Essential Building Blocks and Methodology of Neural Models

1. A scalar input (p) is transmitted through a connection that multiplies its strength by the scalar weight (w), to form the product $w*p$, again a scalar.
2. The transfer function net input (n), again scalar, is the sum of the weighted input $w*p$ plus an optional bias (b). This sum is the argument of the transfer function (f).
3. A transfer function, typically a sigmoid function or a linear function, that takes the argument n and produces the scalar output, a .

During the feedforward process the input vector elements enter the network through the weight matrix \mathbf{W} . The corresponding bias matrix \mathbf{b} is added to the weights generating the net input, n . Appendix D contains the networks weight and bias outputs of all the aircraft used in this research.

$$\mathbf{W} = \begin{bmatrix} w_{1,1} & w_{1,2} & \bullet & w_{1,R} \\ w_{2,1} & w_{2,2} & \bullet & w_{2,R} \\ \bullet & \bullet & \bullet & \bullet \\ w_{S,1} & w_{S,2} & \bullet & w_{S,R} \end{bmatrix}, \quad \mathbf{b} = \begin{bmatrix} b_{1,1} \\ b_{2,1} \\ \bullet \\ b_{S,1} \end{bmatrix}$$

For easy association, row indices of the elements of the matrix \mathbf{W} and \mathbf{b} indicate the destination neuron associated with that weight and bias, while the column indices indicate the source of the input for that weight and bias.

Figure 2 depicts a single layer network of S neurons with multiple input vectors, and shows how the bias effects the net input before going to the transfer function, where the transfer function is contained in the general neuron.

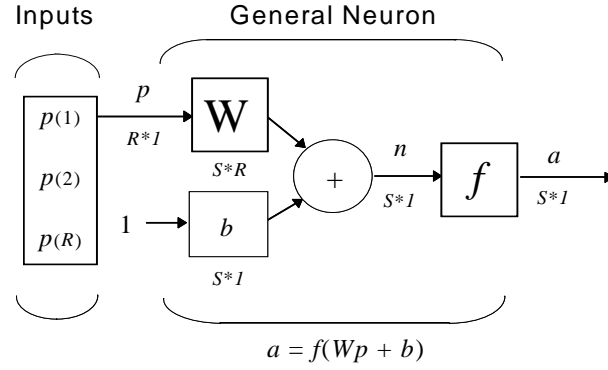


FIGURE 2: Layer of S Neurons with R Inputs

The net input of Figure 2 can be calculated from the summed weight inputs plus a bias to form the equation:

$$n = w_{1,1}p_1 + w_{1,2}p_2 + \dots + w_{1,R}p_R + b .$$

This expression can be written in matrix form:

$$n = Wp + b,$$

where the matrix \mathbf{W} for the single-layer case can have multiple \mathbf{S} neurons in that layer.

The neuron output is calculated as:

$$a = f(Wp + b) .$$

If, for instance, $w_{1,1} = 3$, $p_1 = 2$, $w_{1,2} = 4$, $p_2 = 1$ and $b = -1.5$, then

$$\begin{aligned} a &= f(w_{1,1}p_1 + w_{1,2}p_2 + b) \\ &= f(3(2) + 4(1) - 1.5) \\ a &= f(8.5) \end{aligned}$$

The actual output \mathbf{a} , influenced by the bias, depends on the transfer function. Let it be known that \mathbf{w} and \mathbf{b} are both adjustable scalar parameters of the neuron. Typically,

after the transfer function is chosen the parameters w and b will be adjusted by some learning rule so that the neuron input/output relationship meets some specific goal.

2.6.2 Network Architecture (Hagan *et al.*,1996)

Neurons that receive the same inputs and use the same transfer function may be grouped in layers. Layers of neurons may contain any number of neurons and use any transfer function. Layers may receive input from vectors presented to the network directly or from outputs of other layers. In BP, networks often have one or more layers of sigmoid neurons followed by an output layer of linear neurons. A multiple-layer neural net with nonlinear/linear transfer functions allow the network to learn nonlinear and linear relationships between input and output vectors. A two-layer network with neurons in each layer is shown in Figure 3.

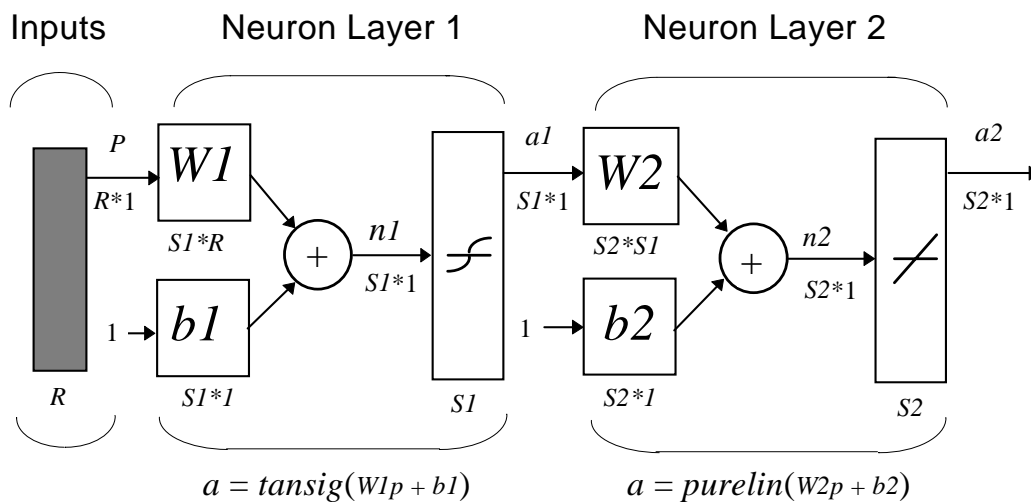


FIGURE 3: Two-Layer Tansig/Purelin Network

Each layer of this network has its own weight matrix, its own bias vector, a net input vector and an output vector. As shown, there are R inputs, S neurons in the first and second layer, where different layers can have different numbers of neurons. For the multiple layer networks it is easy to add the number of the layer to the names of the

matrices and vectors associated with that layer. Hence, the weight matrix and output vector for layer two is denoted as W_2 and a_2 respectively.

This network can be used for general function approximation. It has been proven that two-layer networks, with sigmoid transfer functions in the hidden layer and linear transfer functions in the output layer, can approximate virtually any function of interest to any degree of accuracy, provided a sufficient amount of hidden units are available [Hoescht, 1989]. Therefore, the neuron model key component, the transfer function, is used to design the network and established its behavior. Since a multilayer net is more desirable for this research, the rest of the literature review will be devoted to two-layer neural nets. Now that the basic methodology of the neuron model is stated, lets look at the transfer functions.

2.6.3 Transfer Functions (Hagan *et al.*,1996)

The transfer function may be linear or a nonlinear function of n . And in the case of multiple neurons, there can be linear and/or nonlinear functions, much like the neuron model in Figure 3. A particular transfer function is chosen to satisfy some specification of the problem that the neuron is attempting to solve. There are many common transfer functions, all of which are applied the same way and are capable of handling batches of multiple vectors at a time. Some common transfer functions are listed below:

tansig	hyperbolic tangent sigmoid
purelin	linear
logsig	log sigmoid

The tan-sigmoid transfer function is shown in Figure 4.

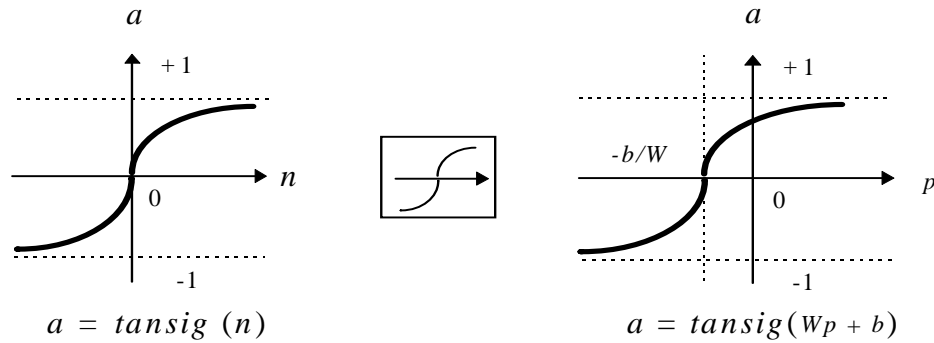


FIGURE 4: Tan-Sigmoid Transfer Function

For example, the following function calculates the output vector \mathbf{a} of a layer of hyperbolic tangent sigmoid neurons given a network input vector \mathbf{p} , the layer's weight matrix \mathbf{W} and bias vector \mathbf{b} , and denote by

$$\mathbf{a} = \mathbf{tansig}(\mathbf{W}\mathbf{p} + \mathbf{b}).$$

This transfer function takes the input vector of any value between plus and minus infinity, and squashes the output into the range -1 to 1, according to the expression:

$$a = \frac{e^n - e^{-n}}{e^n + e^{-n}}.$$

The linear transfer function purelin has output equal to its input, according to the expression:

$$\mathbf{a} = \mathbf{n}.$$

If the last layer of a BP network has sigmoid neurons then the outputs of the network are limited to a small range. If linear output neurons are used the network outputs can take on any value.

The tansig/purelin transfer functions are differentiable and they are also monotonic increasing functions. Differentiable indicates that if the derivative of the

function a exists, then the function is differentiable at a . That is, the derivative of the transfer function must exist at all net outputs, and be monotonic because the output of each function increases as its input increases. Thus, the transfer functions have no minima, which would tend to cause error minimum that could trap the network as it learned.

2.6.4 Backpropagation (Hagan *et al.*,1996)

One of the primary concerns pertaining to this research was trying to decide which learning algorithm would be best for the fuel consumption neural net model. The answer was BP. A basic reference on this subject is “Learning Internal Representations by Error Propagation”, Rumelhart *et al.*, 1986.

BP was created by generalizing the Widrow-Hoff learning rule (Widrow-Hoff, 1960) known as the *delta rule* or the Least Mean Square (LMS) method, where it involves gradient descent techniques in which the performance index is *mean square error* (MSE). Gradient descent is the technique where parameters such as weight and biases are moved in the opposite direction to the error gradient. Each step down the gradient results in smaller errors until an error minima is reached. During training, the network parameters (weights and biases) are adjusted in an effort to optimize the “performance” of the network. A performance surface is created through optimization containing the minima and maxima points generated by the function parameters. The rule is an illustration of supervised training, where the net learns in the presence of a “teacher”. The teacher is based on the level of hidden layers that’s responsible for learning an associative map between the input level and the output level. The input is taught to accommodate changes and appropriately alter the output layer. As each input is applied to the net, the network output is compared to the target. The algorithm will adjust the weights and biases of the net in order to minimize the MSE, where the error is the difference between the target output and the network output. Hence, the rule is applied to a set of pairs of input and target output patterns being associated.

The schematics developed in “Competitive Learning: From Interactive Activation to Adaptive Resonance”, S. Grossberg, 1987, for the BP model is represented in Figure 5. Grossberg’s architecture indicates learning proceeds as follows. Inputs at the first layer (inputs will be considered a layer for architectural purposes) **F1** go through the second layer **F2** and generate outputs at **F3**. While simultaneously, the expected outputs are being fed (by an external teacher) to an error signal **F4**, where the difference between the expected output and the actual output, multiplied by the derivative of the actual output, generate a different error signal **F5**. This error signal is used to change the weights in **F2-F3** pathways. These weights are then communicated to **F4-F5** pathways where they are multiplied by the **F4** error signals to generate weighted error signals at **F5**. These, appropriately weighted by derivatives as in the layers above, are then used to alter the weights in the **F1-F2** pathways. Note that the requirement that the outputs be converted to derivatives of outputs at each layer. Hence layers **F6** and **F7** adds to the complexity of the entire scheme.

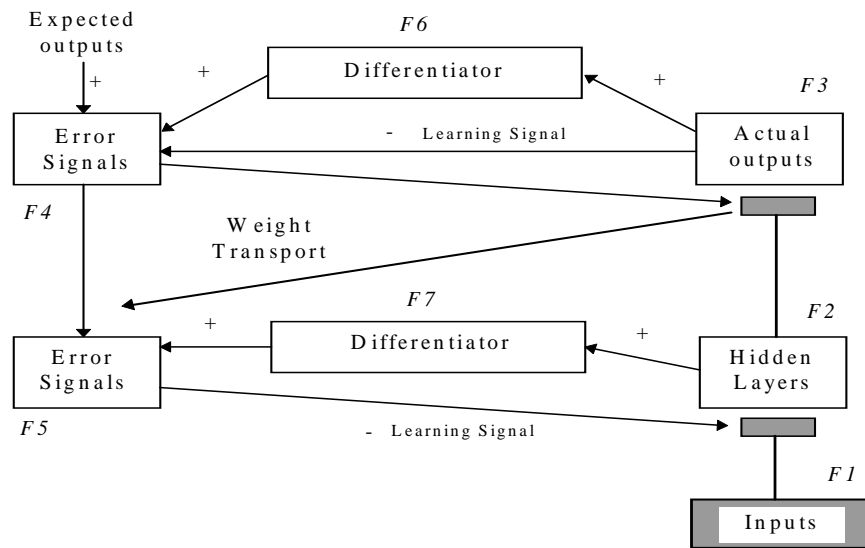


FIGURE 5: BP Learning Schematics

From Grossberg, S. (1987). “Competitive Learning: From Interactive Activation to Adaptive Resonance,” *Cognitive Science*, 11, 23-63.

Much like the LMS, BP differs only in the way the error derivatives are calculated. For the multi-layered case the relationship between the network weights and error is an indirect function of the weights in the hidden layers, they are not directly proportional. In order to calculate the derivatives the chain rule of calculus is needed (See Saltz, 1974). Typically, a new input will lead to an output similar to the correct output for input vectors used in training that are similar to the new input being presented. This can be termed a generalization property which makes it possible to train a network on a representative set of input/target pairs and get satisfactory results without training the network on all possible input/output pairs.

When using the normal BP algorithm, it was determined that it was not sufficient enough to train and produce an acceptable level of computation. The algorithm when applied to the large sets of data developed poor results and lengthy training times. Therefore a variation of the BP was used and called the Levenberg-Marquardt Backpropagation (LMBP).

2.6.5 Levenberg-Marquardt Backpropagation Algorithm (Hagan et al.,1996)

Training feedforward BP neural nets to minimize mean squared errors is a numerical optimization technique. The LMBP is a powerful optimization technique was introduced to the neural net research because it provided methods to accelerate the training and convergence of the algorithm (Scales, 1985). LMBP is a variation of Newton's method that was designed for minimizing functions that are sums of squares of other nonlinear functions. It utilizes the BP procedures in which derivatives are processed from the last layer of the network to the first. Like the variation from LMS to BP, BP's variation to LMBP differs between the way in which the resulting derivatives are used to update weights. This algorithm is well suited for neural net training where the performance index is the MSE.

Developed hundreds of years ago by scientists and mathematicians, the basic principles of optimization were rediscovered to be implemented on high speed computers. In conjunction with the optimization theory, neural nets apply the theory to their training

process. Optimization is an important part of LMBP. The LMBP algorithms role is to optimize a performance index $F(x)$ or find the value of \mathbf{x} that minimizes $F(x)$. In general the optimization begins with some initial guess, \mathbf{x}_0 and then updated versions of the guess through iterations are found according to an equation of the form

$$\mathbf{x}_{k+1} = \mathbf{x}_k + \alpha_k \mathbf{p}_k , \quad (2.26)$$

or

$$\Delta \mathbf{x}_k = (\mathbf{x}_{k+1} - \mathbf{x}_k) = \alpha_k \mathbf{p}_k .$$

where the vector \mathbf{p}_k represents a search direction and the learning rate, α_k , which determines the length of the step.

For this research the value \mathbf{x} that minimizes $F(x)$ is given by the input vectors and biases (performance index; PI)

The Methods to Accelerate the Convergence of Standard BP

- Enhanced Optimizing Techniques
 - Approximate Steepest Descent Rule
 - Gauss-Newton Method

Once the optimum (minimum) point of \mathbf{x} that minimizes the $F(x)$ is found by Eq. 2.26, its desired to have the $F(x)$ decrease at each iteration. In other words,

$$F(\mathbf{x}_{k+1}) < F(\mathbf{x}_k) . \quad (2.27)$$

In order for the “descent” to occur, \mathbf{p}_k must interact with a small learning rate, α_k . The first-order-Taylor series is used as follows

$$F(\mathbf{x}_{k+1}) = F(\mathbf{x}_k + \Delta \mathbf{x}_k) = F(\mathbf{x}_k) + \mathbf{g}_k^T \Delta \mathbf{x}_k ,$$

where: \mathbf{g}_k^T is the gradient evaluated at the first value of \mathbf{x} that minimizes the $F(\mathbf{x})$.

The gradient vector:

$$\mathbf{g}_k = \nabla F(\mathbf{x}) \Big|_{\mathbf{x}=\mathbf{x}_k} . \quad (2.28)$$

To satisfy Eq. 2.27 the second term on the right hand side of Eq. 2.28 must be negative

$$\mathbf{g}_k^T \Delta \mathbf{x}_k = \alpha_k \mathbf{g}_k^T \mathbf{p}_k < 0 .$$

In general it is best to select a small learning rate, α_k , as this will improve the search direction.

This implies:

$$\mathbf{g}_k^T \mathbf{p}_k < 0 .$$

Therefore, using this logic along with the iteration of Eq. 2.26 produces the *steepest descent method*:

$$\mathbf{x}_{k+1} = \mathbf{x}_k - \alpha_k \mathbf{g}_k^T .$$

The Gauss-Newton method is based on the second-order Taylor series. This method will always find the minimum of a quadratic function in one step. It is designed to approximate a function as quadratic and then locate the stationary point of the quadratic approximation. If the original function is quadratic (with a strong minimum) it will be minimized in one step. If the original function $F(\mathbf{x})$ is *not* quadratic then the method will not generally converge in one step.

Second-order Taylor series:

$$F(\mathbf{x}_{k+1}) = F(\mathbf{x}_k + \Delta \mathbf{x}_k) = F(\mathbf{x}_k) + \mathbf{g}_k^T \Delta \mathbf{x}_k + 1/2 \Delta \mathbf{x}_k^T \mathbf{A}_k \Delta \mathbf{x}_k , \quad (2.29)$$

Use $\nabla F(x) = Ax + d$ to take the gradient of Eq. 2.29 with respect to Δx_k and set it equal to zero to get $g_k + A_k \Delta x_k = 0$.

Solving for Δx_k produces

$$\Delta x_k = -A_k^{-1} g_k.$$

Newton's method for optimizing a performance index $F(x)$ is

$$x_{k+1} = x_k - A_k^{-1} g_k. \quad (2.30)$$

where $A_k \equiv \nabla^2 F(x)|_{x=x_k}$ and $g_k \equiv \nabla F(x)|_{x=x_k}$.

If we assume that $F(x)$ is the sum of squares function:

$$F(x) = \sum_{i=1}^N v_i^2(x) = v^T(x)v(x),$$

then the j^{th} element of the gradient would be

$$[\nabla F(x)]_j = \frac{\partial F(x)}{\partial x_j} = 2 \sum_{i=1}^N v_i(x) \frac{\partial v_i(x)}{\partial x_j}.$$

The gradient can therefore be written in matrix form:

$$\nabla F(x) = 2\mathbf{J}^T(x)v(x). \quad (2.31)$$

where \mathbf{J} is the Jacobian matrix and depicted as

$$\mathbf{J}(\mathbf{x}) = \begin{bmatrix} \frac{\partial v_1(\mathbf{x})}{\partial x_1} & \frac{\partial v_1(\mathbf{x})}{\partial x_2} & \dots & \frac{\partial v_1(\mathbf{x})}{\partial x_n} \\ \frac{\partial v_2(\mathbf{x})}{\partial x_1} & \frac{\partial v_2(\mathbf{x})}{\partial x_2} & \dots & \frac{\partial v_2(\mathbf{x})}{\partial x_n} \\ \vdots & \vdots & & \vdots \\ \frac{\partial v_N(\mathbf{x})}{\partial x_1} & \frac{\partial v_N(\mathbf{x})}{\partial x_2} & \dots & \frac{\partial v_N(\mathbf{x})}{\partial x_n} \end{bmatrix}.$$

The next step is finding the Hessian matrix. The k,j element of the Hessian matrix would be

$$[\nabla^2 F(\mathbf{x})]_{k,j} = \frac{\partial^2 F(\mathbf{x})}{\partial x_k \partial x_j} = 2 \sum_{i=1}^N \left\{ \frac{\partial v_i(\mathbf{x})}{\partial x_k} \frac{\partial v_i(\mathbf{x})}{\partial x_j} + v_i(\mathbf{x}) \frac{\partial^2 v_i(\mathbf{x})}{\partial x_k \partial x_j} \right\}.$$

The Hessian matrix can then be expressed in matrix form:

$$\nabla^2 F(\mathbf{x}) = 2\mathbf{J}^T(\mathbf{x})\mathbf{J}(\mathbf{x}) + 2\mathbf{S}(\mathbf{x}),$$

where

$$\mathbf{S}(\mathbf{x}) = \sum_{i=1}^N v_i(\mathbf{x}) \nabla^2 v_i(\mathbf{x}).$$

If we assume that $\mathbf{S}(\mathbf{x})$ is small, we can approximate the Hessian matrix as

$$\nabla^2 F(\mathbf{x}) \cong 2\mathbf{J}^T(\mathbf{x})\mathbf{J}(\mathbf{x}). \quad (2.32)$$

By substituting Eq. (2.32) and Eq. (2.31) into Eq. (2.30), we obtain the *Gauss-Newton* method:

$$\begin{aligned} \mathbf{x}_{k+1} &= \mathbf{x}_x - \left[2\mathbf{J}^T(\mathbf{x}_k)\mathbf{J}(\mathbf{x}_k) \right]^{-1} 2\mathbf{J}^T(\mathbf{x}_k)\mathbf{J}(\mathbf{x}_k). \\ &= \mathbf{x}_x - \left[\mathbf{J}^T(\mathbf{x}_k)\mathbf{J}(\mathbf{x}_k) \right]^{-1} \mathbf{J}^T(\mathbf{x}_k)\mathbf{J}(\mathbf{x}_k) \end{aligned}$$

Note that the advantage of Gauss-Newton over the standard Newton's method is that it does not require calculation of second derivatives. The first derivatives are applied to the Hessian matrix at each iteration and then inverted. A process to insure that the matrix can be inverted modifies the approximate Hessian matrix. This is done through the use of eigenvalues. The eigenvalues of the matrix are tested to check if the condition of the Hessian matrix is positive. The first order Jacobian matrix is implemented into the Hessian matrix and treated as a second order partial differentiation. The eigenvalue relation is denoted by:

$$\mathbf{G} = \mathbf{H} + \mu\mathbf{I}.$$

Where the hypothetical eigenvalues and eigenvectors of \mathbf{H} are $\{\lambda_1, \lambda_2, \dots, \lambda_n\}$ and $\{z_1, z_2, \dots, z_n\}$. Then,

$$\mathbf{Gz}_i = [\mathbf{H} + \mu\mathbf{I}]\mathbf{z}_i = \mathbf{Hz}_i + \mu\mathbf{z}_i = \lambda_1 z_1 + \mu z_1 = (\lambda_i + \mu)\mathbf{z}_i.$$

Hence, the eigenvectors of \mathbf{G} are "equal" to those of \mathbf{H} . \mathbf{G} can be made positive definite by increasing μ until $(\lambda_i + \mu) > 0$ for all i , and therefore the matrix will be inverted. A positive definitive Hessian matrix is a second-order, sufficient condition for a strong minimum to exist.

Iterations of the LMBP Algorithm (Scales, 1985):

1. Present all inputs to the network and compute the corresponding network outputs by
 - propagating the input forward through the net:

$$\mathbf{a}^0 = \mathbf{p}_g ,$$

$$\mathbf{a}^{m+1} = \mathbf{f}^{m+1}(\mathbf{W}^{m+1} \mathbf{a}^m + \mathbf{b}^{m+1}), \text{ for } m = 0, 2, \dots, m-1 ,$$

$$\mathbf{a} = \mathbf{a}^m .$$

- propagate the sensitivities backward through the network:

$$\mathbf{s}^m = -2\dot{\mathbf{F}}^m(\mathbf{n}^m)(t - a),$$

$$\mathbf{s}^m = \dot{\mathbf{F}}^m(\mathbf{n}^m)(\mathbf{W}^{m+1})^T \mathbf{s}^{m+1}, \text{ for } m = m-1, \dots, 2, 1.$$

- update weights and biases using the approximate steepest descent rule:

$$\mathbf{W}^m(k+1) = \mathbf{W}^m(k) - \alpha \mathbf{s}^m (\mathbf{a}^{m-1})^T,$$

$$\mathbf{b}^m(k+1) = \mathbf{b}^m(k) - \alpha \mathbf{s}^m .$$

- compute the corresponding network errors:

$$\mathbf{e}_q = (t_q - a_q)^m$$

- compute the sum of squared errors over all inputs, $F(x)$, using the following logic:

If each target occurs with equal probability, the MSE is proportional to the sum of squared errors over the Q targets in the training set:

$$\begin{aligned} F(x) &= \sum_{q=1}^Q (t_q - a_q)^T (t_q - a_q) \\ &= \sum_{q=1}^Q \mathbf{e}_q^T \mathbf{e}_q = \sum_{q=1}^Q \sum_{j=1}^{s^m} (e_{j,q})^2 = \sum_{i=1}^N (v_i)^2, \end{aligned}$$

where $e_{j,q}$ is the j^{th} element of the error for the q^{th} input/target pair.

2. The key step in the LMBP algorithm is the computation of the Jacobian matrix. To create the matrix we need to compute the derivatives of the errors.

- the form of the matrix is presented by a parameter vector:

$$\mathbf{x}^T = [\chi_1 \chi_2 \dots \chi_n] = [w_{1,1}^1 w_{1,2}^1 \dots w_{S^1,R}^1 b_1^1 \dots b_{S^1}^1 w_{1,1}^2 \dots b_{S^2}^2 \dots w_{1,1}^M \dots b_{S^M}^M],$$

$$N = Q \times S^M \text{ and } n = S^1(R + 1) + S^2(S^1 + 1) + \dots + S^M(S^{M-1} + 1).$$

and an error vector:

$$\mathbf{v}^T = [v_1 v_2 \dots v_n] = [e_{1,1} e_{2,1} \dots e_{S^M,1} e_{1,2} \dots e_{S^M,Q}].$$

- calculate the sensitivities with the recurrence relations:

The BP process computes the sensitivities through a recurrence relationship from the last layer backward to the first layer. When the input \mathbf{p}_q has been applied to the network and the corresponding output \mathbf{a}_q^M has been computed, the LMBP is initialized with

$$\tilde{\mathbf{S}}_q^M = -\dot{\mathbf{F}}^M(n_q^M),$$

where: $\dot{\mathbf{F}}^M(n_q^M)$ is the matrix of the function, \mathbf{f} , that is an explicit function only of the variable \mathbf{n} .

$$\dot{\mathbf{F}}^M(n^M) = \begin{bmatrix} \dot{f}(n_1^M) & 0 & \dots & 0 \\ 0 & \dot{f}(n_2^M) & \dots & 0 \\ \vdots & \vdots & \dot{f}(n_3^M) & \vdots \\ 0 & 0 & 0 & \dot{f}(n_{S^M}^M) \end{bmatrix}$$

Each column of the matrix $\tilde{\mathbf{S}}_q^M$ must be backpropagated through the net using the final recurrence relation for the sensitivity: Using the Chain rule in matrix form and denoted as

$$\tilde{\mathbf{S}}^M = \frac{\partial \hat{\mathbf{F}}}{\partial n^M} = \left(\frac{\partial n^{M+1}}{\partial n^M} \right)^T \frac{\partial \hat{\mathbf{F}}}{\partial n^{M+1}} = \dot{\mathbf{F}}^M(n^M)(\mathbf{W}^{M+1})^T \frac{\partial \hat{\mathbf{F}}}{\partial n^{M+1}},$$

Therefore to produce one row of the Jacobian matrix, the columns can be BP together using:

$$\tilde{\mathbf{S}}_q^M = \dot{\mathbf{F}}^M(n^M)(\mathbf{W}^{M+1})^T \tilde{\mathbf{S}}^{M+1}.$$

The total Marquardt sensitivity matrices for each layer are created by augmenting the matrices computed for each input:

$$\tilde{\mathbf{S}}^M = \left[\tilde{\mathbf{S}}_1^M | \tilde{\mathbf{S}}_2^M | \dots | \tilde{\mathbf{S}}_Q^M \right].$$

Note that for each input the net will backpropagate S^M sensitivity vectors. This is because derivatives are computed for each individual error, rather than the derivative of the sum of squares of the errors. For every input applied to the net there will be S^M errors, for each error, there will be one row of the Jacobian matrix.

$$\mathbf{J}(\mathbf{x}) = \begin{bmatrix} \frac{\partial e_{1,1}}{\partial w_{1,1}^1} & \frac{\partial e_{1,1}}{\partial w_{1,2}^1} \dots & \frac{\partial e_{1,1}}{\partial w_{S^1,R}^1} & \frac{\partial e_{1,1}}{\partial b_1^1} \dots \\ \frac{\partial e_{2,1}}{\partial w_{1,1}^1} & \frac{\partial e_{2,1}}{\partial w_{1,2}^1} \dots & \frac{\partial e_{2,1}}{\partial w_{S^1,R}^1} & \frac{\partial e_{2,1}}{\partial b_1^1} \dots \\ \vdots & \vdots & \vdots & \vdots \\ \frac{\partial e_{S^M,1}}{\partial w_{1,1}^1} & \frac{\partial e_{S^M,1}}{\partial w_{1,2}^1} \dots & \frac{\partial e_{S^M,1}}{\partial w_{S^1,R}^1} & \frac{\partial e_{S^M,1}}{\partial b_1^1} \dots \\ \frac{\partial e_{1,2}}{\partial w_{1,1}^1} & \frac{\partial e_{1,2}}{\partial w_{1,2}^1} \dots & \frac{\partial e_{1,2}}{\partial w_{S^1,R}^1} & \frac{\partial e_{1,2}}{\partial b_1^1} \dots \\ \vdots & \vdots & \vdots & \vdots \end{bmatrix}.$$

- compute the elements of the Jacobian matrix by

$$[\mathbf{J}]_{h,l} = \frac{\partial v_h}{\partial x_l} = \tilde{s}_{i,h}^M \times a_{j,q}^{m-1},$$

or if x_l is a bias,

$$[\mathbf{J}]_{h,l} = \frac{\partial v_h}{\partial x_l} = \tilde{s}_{i,h}^M.$$

3. Solve the LMBP algorithm.

- solve $\Delta \mathbf{x}_k$:

$$\Delta \mathbf{x}_k = -[\mathbf{J}^T(\mathbf{x}_k)\mathbf{J}(\mathbf{x}_k) + \mu_k \mathbf{I}]^{-1} \mathbf{J}^T(\mathbf{x}_k) \mathbf{v}(\mathbf{x}_k),$$

or

$$\Delta \mathbf{W} = (\mathbf{J}^T \mathbf{J} + \mu \mathbf{I})^{-1} \mathbf{J}^T \mathbf{e}.$$

where the step multiplier, μ is a scalar, and \mathbf{e} is an error vector. If μ is very large, the above expression approximates a gradient descent method, while if it is small the above expression becomes the Gauss-Newton method. Because this second method is faster and

more accurate near an error minimum so the aim is to shift towards the Gauss-Newton method as quickly as possible. Thus, μ is decreased after each successful step and increased only when a step increases the error.

4. Recompute the sum of squared errors using $(x_k + \Delta x_k)$. If the sum of squares is smaller than that of step 1, divide μ by a step multiplier factor, ϑ , let $x_{k+1} = x_k + \Delta x_k$ and go back to step 1. If the sum of squares is not reduced, then multiply μ by ϑ and go back to step 3.

The LMBP algorithm converges when the norm of the gradient is less than the predetermined value or when the sum of squares has been reduced to some error goal.

The main draw back of LMBP is the storage requirement. The $J^T J$ matrix, which must be inverted, is $n \times n$, where n is the total number of weights and biases in the network. If the network has more than a few thousand parameters, the LMBP algorithm becomes impractical on current computers.

3. METHODOLOGY

3.1 *Introduction*

This chapter describes the methodology used for conducting this research. The main objective of the methodology is to develop a realistic, easily implemented, efficient method for fuel consumption modeling through neural network applications. With the use of optimization, finding the value of weights and biases that minimize the $F(x)$, where x is the scalar parameter (composed of two variables) that is adjusted each time the neural net iterates, a model can be developed to calculate fuel consumption at any velocity and altitude desired. This chapter briefly describes the development of the fuel consumption model, the neural network, the approach to efficient neural networking, and the use of MATLAB as an optimization tool.

3.2 *Models and Nonlinear Optimization*

The first step in studying fuel consumption is to identify past techniques used to model fuelburn of an aircraft. Once this is established the researcher can relate past techniques with his/her own logic to formulate and build a model. Concisely, a model can be thought of as a representation of parts that when combined and work with each other create a whole, in this case the whole is fuel consumption. A model is used to investigate possible improvements of the study, and discover the effect of different inputs that could alter the output. There are many kinds of models. For example, verbal-descriptive, graphical, mathematical, logical algorithms and computer models. In certain instances a given study may be best modeled by a culmination of these types. Because of the need to incorporate numerical data and logic, this fuel consumption model is almost invariably mathematical and logical algorithm based, and the analysis employs both methods.

A model's directive is to satisfy an objective as the purpose of the study. It should be highly faithful in representing the objective, accurately reproducing its outcome or predicting the results of hypothetical application. A valid point to make is that a model can comprise subsystems (submodels) in order to reduce the complexity because submodels are often easier to define. Good model performance also relies on the level of detail and nonambiguity of the model.

The model, a neural network fuel consumption model (AFCM), will be compared to the SIMMOD fuelburn post-processor. It will incorporate two submodels: (1) the AFBM, (2) a multilayer neural network optimization model (NNOM).

Nonlinear optimization is used because of the nonlinearity of the transfer functions. This technique, sometimes called continuous-variable nonlinear programming, involves real decision variables but the objective and constraint functions are not necessarily linear. The objective of optimization is to train the network parameters (w , b) so they can be adjusted in an effort to optimize the performance of the network. Neural nets are taught to accommodate changes in the weights and bias to appropriately reconfigure the output. Each time it iterates (teaches), the error between the output and target becomes smaller until a minimized error goal is achieved. The theoretical outlook for the AFCM should be as follows:

- goal or purpose directed
- understandable and easy to use
- suitable for a wide range of aircraft
- easy to modify or update the model

The whole idea for this research stemmed from SIMMOD. Looking for ways to make the software operate more efficiently incorporating a different approach in calculating fuelburn. For this model to be useful the above statement must be satisfied including the ability for the model to be implemented into SIMMOD or any airport/airspace simulation software. Although the model is not dynamic in nature relative

to SIMMOD's AFBM, it can be incorporated into the software so that it will be recognized to compute fuelburn at every point in the flight path.

3.3 Approach to Model Development

A successful study is related to the methodology used by the modeller and his/her knowledge of the platform and expertise in the analysis of the topic in question. It is usually better to have a plan before starting modeling. The following activities or steps are applied in this research to compose a sound fuel consumption model.

- *Problem Formulation.* Successful problem formulation is the most critical step in developing a model. The first issue is to bound the problem, to gather all the information critical to the overall objective.

- *Data Collection and Analysis.* Information and data needed by the fuel consumption model should be identified and collected. The data needed is

Specific Aircraft Coefficients that come from Bela Collins AFBM

Velocity, Altitude and Fuelflow generated from the AFBM

All parameters and variables that affect the measure of fuelburn such as atmospheric properties are also to be identified. The AFBM will be the base model that the neural network will try to map. Once that is done the neural net will generalized fuel consumption data within the parameters defined by the base model. After the generalization process the new data is then implemented back into the base model to be compared with the generalized data. If the data comparison is a success then fuel consumption can be estimated at specific velocities and altitudes for that particular aircraft.

- *Model Development.* The AFCM consists of two major subsystem models: The AFBM, which performs the initial fuel consumption calculations and termed the

“fuelburn calculator”, and the NNOM, which utilizes the initial velocity, altitude and fuel consumption data from the AFBM to mimic the fuel consumption.

In order to formulate the subsystem models into the AFCM an explicit approach is used to analyze each segment of the models. This method is used to define the individual algorithms or information entities through the model on the basis of sequence of events that occur in a pre-defined pattern.

This research can be broadly divided into two parts: (1) determining a velocity and altitude profile that generates fuel consumption, and (2) invoking that data into a well defined neural network. The detail of this logic will be presented in Chapter 4. After formulation the subsystem models will be tested together in the MATLAB environment. The next step is to combine the models to form a single model (AFCM). It is necessary for the modeller to chose aircraft specific data that corresponds to the desired aircraft being modeled. It maybe useful to run the AFBM with the selected aircraft data in order to verify the accuracy of the model before combining it with the NNOM. In this step, it is also important to delete any ambiguity within the data output. For example, if the output shows that the aircraft travels at some velocity and altitude consuming fuel at an unbelievable rate, then these outliers can be removed from the data base. The following represents an example of the ambiguous case:

Type Aircraft: MD-80
Velocity: 500 knots (IAS)
Altitude: 44,000 feet

It would not be feasible for this aircraft to travel at these parameters.

- *Validation and Modification of Models.* The validity of models is a measure of the extent to which the parameters satisfy the study objectives. Validation involves conducting a series of tests on the input, output, and structure of the model. Common methods for validating are to compare the output of the model(s) to initial data under similar environmental conditions and to check the reliability of the output. Basically, if the output is similar the final model is accepted as a realistic representation for the

research. The following output from the AFCM is used as a measure of effectiveness for comparison with the generalized AFBM output data: (1) the mean, (2) root-mean-square (RMS), (3) t-test, (4) confidence interval, and (5) the computation time of the entire AFBM fuel consumption output compared to the AFCM fuel consumption output. The ultimate validation of the AFCM is how well it can predict the fuel consumption of an aircraft with specific input parameters (velocity and altitude).

- *Design Experiments and Running the Optimization.* In this step it must be decided what aircraft input variables, and neural net structure to use for the design of the AFCM. An experimental design requires observations of the submodels under specific combinations run in the MATLAB environment. For a selected AFCM, some decisions must be made on certain issues as initial conditions for the AFBM, the neural net design architecture, and encompassing neural net design parameters. Once these are met the AFCM can be tested and used in actual aircraft specific scenarios.

- *Analysis of Output Data and Implementation.* Analysis of the AFCM results is to achieve the research objectives. This step brings out several important outcomes such as determination of fuel consumption at a particular point within the flight envelope, the floating point operations (flops) of the AFBM compared to the neural nets generalization, and the accuracy of the neural net generalization compared to the generalized AFBM (GAFBM). The analyst draws inferences from these outcomes and makes specific recommendations on how the AFCM works and how it could be improved. This is not a simple process, at a number of points the process may go back to the previous step.

3.4 Aircraft Fuel Consumption Model (AFCM) Assumptions

The AFCM assumptions are based on simplifying the energy balance equation. By simplifying the equation we get **point** performance. As stated, the model has been modified to except only the cruise segment of the profile. With this in mind several of the assumptions were left out, such as the climb/descent rates and incremental changes in altitude of approximately 2,000 ft or approximately 200 seconds during level flight.

During level cruise the following is assumed in order to maintain efficient computations without an unacceptable effect on accuracy:

1. The aircraft weight change at a certain flight level is small compared to the total weight, therefore total weight is used in the calculations.
2. Acceleration = 0 during any flight level.
3. The flight path angle (γ) is small, therefore $\cos\gamma \cong 1$, or the aircraft weight equals the required lift.
4. Upper wind effects on fuel consumption are not a part of the computational requirement; therefore the velocity [IAS] equals the ground speed.
5. The functional forms used for lift vs. drag, and thrust over fuel flow, are sufficient to obtain a good data fit over the desired speed range.
6. The standard US atmospheric conditions apply.

3.5 Description of MATLAB

MATLAB, created by MathWorks Inc. is a powerful and advanced computational software that handles numeric computation, algorithm prototyping and specific purpose problem solving with matrix formulations that arise in disciplines such as optimization and statistics. MATLAB is used for research, solving practical engineering and mathematical problems. MATLAB 4.0 is the current version of MATLAB used in a variety of platforms for today's systems. An updated version 5.0 is due to come out some time in early 1997. This software has powerful features used toward an array of disciplines. The toolboxes within MATLAB give this software the versatility needed for today's high demand in programming, simulation, and graphing.

A MATLAB NNOM consists of input vectors, target vectors, transfer functions, learning rates, and sum-square error goals. All of which are very easy to modify and manipulate. Also to test the sensitivity of the model and have the possibility to

incorporate a graphical user interface (GUI). The following features of MATLAB that are pertinent to this research are as follows:

1. Solving problems in a fraction of the time it takes to write another program in another language to produce the same output.
2. Extensive toolboxes to solve particular classes of problems.
3. Easily extensive, allowing you to be the author of the programming, creating your own applications.
4. Interaction with other programming languages (Fortran, C++).
5. Hierarchical modeling to make complex systems easy to build and understand.
6. On-line help is available from help commands at the MATLAB prompt, and technical service assistance via e-mail at tech@mathworks.com

The powerful features of MATLAB prove to be effective in this research.

3.6 Research Discussion and Pertaining Questions

Modeling software - MATLAB has extensive neural net capabilities. The neural net is similar to the polynomial approximation structure except the weights of each coefficient can have specific ways of behaving through the use of a multitude of sigmoid or linear transformations. Neural networks can contain a series of neurons that possess input and output layers, where each neuron will have a specific weight coefficient and bias coefficient. Suppose the neural net contains input variables P_1 and P_2 , they effect fuel consumption by drag forces that are related to the amount of thrust. The output will be fuel flow, although there can be multiple outputs such as fuel flow and thrust. This research only requires one output: fuel flow. The aircraft must be kept under certain conditions, meaning it can move with three degrees of freedom, require certain velocities and altitudes based on a specific fuel flow.

The neural net design raises few questions/decisions:

- Decide on the structure, what rules apply? The structure of the network contains input vectors and target vectors from a base algorithm (AFBM). Using function approximation and generalization the output data can be obtained and compared to the GAFBM. Function approximation is one of the most powerful uses of a neural network. The typical two layer architecture used for a function approximation network involves a hidden layer of sigmoidal neurons which receive inputs directly and then broadcast their outputs to a layer of linear neurons which compute the network output. This architecture has been proven to be capable of approximating any function with finite number of discontinuities with arbitrary accuracy. In general, a more complex function requires more sigmoidal neurons in the hidden layer. The question is can we approximate the non linear function, fuel flow?

- Decide on the coefficients weight, W . The weights and biases are defined when the net introduces the input vectors. The input vectors will be normalized randomly generated values ranging from zero to one.

- What topology? Meaning how many neurals per layer, how many layers? For example, when designing an urban network, how many streets are needed to move a certain volume of traffic? The more layers, the more complicated it gets, the more time to train. Hence, the more "fine tuned" it gets. The goal is to optimize the topology if applicable. At this point in time the optimal topology will be a two layer tansig/purelin network. The first layer performs the hyperbolic tangent sigmoid functions, while the last layer performs the pure linear functions.

The structure of the neural net is depicted below:

600-7-1

where 600 is the number of inputs, 7 is the number of neurons per layer, and 1 for the single neuron in the output layer.

- What transfer functions should be used? The type of transfer functions may effect the output. One hyperbolic tansig function and one purelin function will be tested. This was chosen because the extreme capabilities of this function combination. If the last layer of a BP network has sigmoid neurons then the output of the net is limited to a small range of values. If a linear output neuron is used the network output can take on any value.

- What type of algorithms? Backward Propagation was the first thought. Then after researching all the algorithms the most efficient approach was found to be LMBP. This algorithm dramatically enhances the systems computation. Below is a comparison of three supervised functions produced by one of the many demos that MATLAB has to offer and run on a Macintosh Quadra 950.

Function	Technique	Time*	Flops
TRAINBP	Backpropagation	259.1	2.16E+08
TRAINBPX	Faster Backprop	42.4	2.97E+07
TRAINLM	Levenberg-Marquardt	3.3	315769

*Times are in seconds and may vary.

Source: MATLAB Reference Manual, MathWorks Inc., 1992.

Some neural nets, instead of implementing continuous variations, they implement binary variables (zero and one) this type of net is good for discrete decisions. This research involves a system that moves over a continuum of values. Neurons will possess continuous variation, which is the continuum of values. Continuous variation may contain discontinuity in the variation of the neural net due to flap settings. Flap settings are discrete, there may be discrete numbers of the variable that are used in the network. Considering that flaps are not used in this research there is no concern just an idea that could be used in a future model.

The behavior of each neural depends on the transfer function, and when they are combined their behavior could be highly non-linear. Therefore, adjusting the coefficients between these variables and the fuel flow value according to the range of solutions should

satisfy the model. Doing this for each of the nodes, not knowing the outcome. The beauty about this is that the data can be totally non-linear and still be effective. What is the interrelationship between the nodes considering the neurals posses a unique behavior. There is also a causality or behavior pattern within the nodes. How is the connection of the nodes done once the topology is selected? Once the topology is selected it depends on the transfer function, the output of each function is in term the input of the next layer. This input is invoked in each neuron of the new layer. A three layer network with \mathbf{R} rows and \mathbf{Q} columns is shown in Figure 6. The level of computation is in Table 2, Chapter 5.

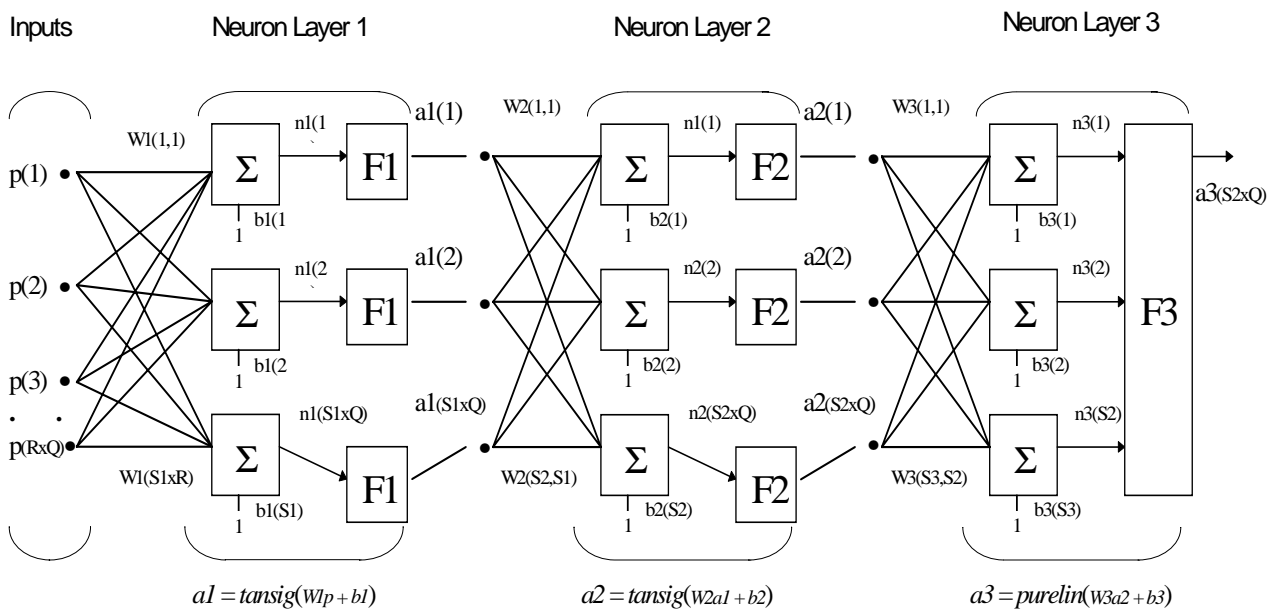


FIGURE 6: Three-Layer Neural Network

The idea of training the network is identify, find or minimize (found by optimization) the \mathbf{W} 's and biases of the dimensional network so that the error in the output is minimized. The data must relate, for example, there are 600 points (data) with two arguments each (Velocity, Altitude), feed the 600 points into the computer and compare what the network is doing with the actual data verses the GAFBM. Do this with a random set of data that fits within the boundaries of the actual data and test until the

discrepancy observed throughout the entire range of values is within a given tolerance. A better tolerance can be achieved by increasing the training cycle. There might be a point where everything reaches a steady state (does not converge). It is only for each neural looking at 3D data. Fuel flow will be plotted, maybe heavily nonlinear. By replicating this idea using neural networks for each condition (similar to regression) the error can be found for the i^{th} point. The training cycle will minimize to a defined sum-square error goal. This is an intriguing non-linear optimization problem.

P values are the normalized values of altitude and velocity. This value physically represents two variables combined but in reality the value is the fuel flow under one condition of altitude and velocity. P is the input vector (X range), and T is the target vector (Y range). T values are dependent variables, and the P values are independent variables. The only way to get this type of behavior in a neural net as a function approximation envelope is to have two variables in one input vector.

The matrix (two rows, 600 columns) consists of an array of numbers, where the X and Y dimension of the array could represent the X and h domain. Then of course you will have another vector or some other array that would represent the value of Y, which in this case is called T (target vector). It is imperative to make sure that the new data fall within a certain margin of error of the existing curves that are used in the training procedure. If it does then that is the assurance needed to accept that the neural net is approximating correctly.

The problem is we don't have the real data. Hence, Collins (1984) algorithm can be used, a different set of inputs should generate different fuel consumption's. This will give a different set of fuel consumption's, different from the ones used to train the net. Then compare the two fuel consumption values by computing the RMS, t-test, and confidence intervals between the neural net result and the actual computation to show how well the data fits together.

As stated before one of the challenges is to compare the polynomial fuelburn function to the neural network so we can understand the accuracy as well as the severity of computation of each function. This is not difficult because in MATLAB at the end of every computation we can obtain the number of floating point operations (flops) that have

occurred. Hence, there can be two algorithms programmed in MATLAB, within the algorithm you can query the number of floating point operations. This will tell you the degree of intensity of the model and then you can compare both models.

It is obvious that the accuracy of the output data can be improved with longer training times. The question is for a real time (fast time) simulation like SIMMOD we need to balance accuracy and speed. Getting within 0.001% accuracy at ten-times the computational intensity or being within 1% of the base data without the computational intensity? It would be best to compare this data with the data that was used when developing the original fuel consumption algorithm because this algorithm is within a maximum of 4% accuracy most of the time. Assuming that this research can derive a simpler neural net structure that might be half as complex as the AFBM in terms of computation capability, and having the error be within one percent because the neural net can always be adjusted to the error by letting the training process go longer, or using more neurals (whatever the case).

Once you use the neural net you have a trained model, you have a multidimensional linear regression equation in the neural net that you can code directly into your airport/airspace program that should be half as computationally intensive as the AFBM.

4. MODEL DESCRIPTION

4.1 Introduction

This chapter concentrates on the NNOM that is found in the AFCM. The model description is intended to present a descriptive presentation of the neural network. The description defines the important neural net components and their interrelationships. Up till now the NNOM has been described in the general sense, where it is the intent to define all the important aspects that lead to the development of the model. The presentation will include the development of the input, inner layers and output transforms.

4.2 Specifics of the Neural Network

Determining the velocity and altitude profiles are extracted from the aircraft speed and altitude envelope at which it normally flies. Each aircraft model has corresponding performance data. The pertinent information is extracted from the SIMMOD, the FAA Airfield and Airspace Simulation Model, aircraft data files and used in the AFCM.

Input/Target Data Format (Beal *et al.* 1992)

The format of the input data will consist of two variables in row vector form. Six-hundred random pieces of data will be assigned to each variable. Therefore the velocity and altitude will have one row vector each containing 600 columns. The target data is a single row vector that is generated by the AFBM using the input data. Figure 7 gives an illustration of the format.

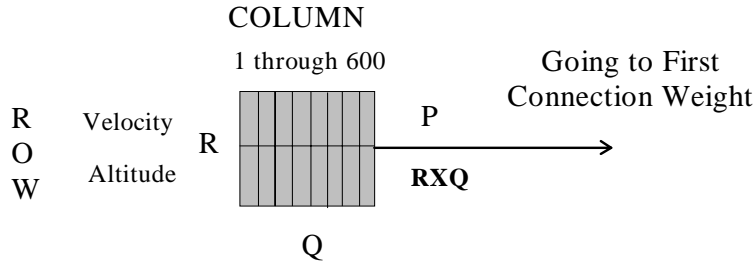


FIGURE 7: Two Dimensional Input Vector

The neural net reads the input vectors and target vectors by the formulation

$$P = [Vkts/O;A/45000;];\% \text{ Inputs,}$$

$$T = Wf/U;\% \text{ Targets,}$$

where the velocity, Vkts (TAS), altitude, A, and fuel consumption, Wf are normalized from zero to one for easier association.

Input Transforms (Beal *et al.* 1992)

There is only one input transform in use in this NNOM. A simple weighting function is used to transform the inputs. The input transformation is given by

$$w_i * p_i ,$$

where w_i is the connection weight, and p_i is the input vector. Because this very simple transform is applied to each connection, neural net technology is commonly referred to a “connectionism”. The w is a weight of the conjunct: a conjunct is a grouping of inputs with indices $i(j)$ conjoined together using the product function. The input transform is sent to the summation function, where the bias (b) term is added to $w p$. The net input, n goes into the transfer function and written as:

$$n = (wp + b).$$

The bias is added to the product (wp) because it keeps the net input within a concise range, eliminating any ambiguity in the product wp .

Output Transforms (Beal *et al.* 1992)

There are a number of output transforms known as transfer functions. The net input is introduced to this function. It is also important to note the architecture of the net, where each layer can have multiple neurons each neuron having different transfer functions. The network architecture for this research will consist of a 600-7-1 network. Having 600 pieces of data allows the net to successfully approximate the functions within each layer. It was tested with many different data sets, both $< 600 <$. Finding that the smaller and larger data sets under and over compensated the learning functions allowing for poor approximation.

The transfer function used throughout the first layer is a hyperbolic tangent sigmoid function. Otherwise known in the MATLAB environment as **tansig**. This function as well as the others mentioned in the literature review only differs in the abruptness of their transitions. The tansig function takes the net input (an integer) and constrains the neuron output, a to some desired range then feeding this output forward to the next layer. The range in question is from -1 to 1. The purpose for the function is to smooth the output so that differentiation can be performed to facilitate the learning process. A tansig function is common in BP networks because it permits adaptation using classical optimization techniques. The neural net requires the user to enter the number of hidden neurons per layer. This is achieved by the following:

$$S1 = 7; \% \text{ Number of hidden neurons in the first layer,}$$

where S1 represent layer one having seven neurons in the first layer and two in the output layer.

The second layer (single neuron) is a linear transfer function known as **purelin**. This function is used because the weights often go outside the range of the previous function. The reason for this is that finite numbers of discontinuities can come from the previous function. Therefore, if the last layer of a BP net has sigmoid neurons then the output of the net are limited to a small range. If the linear output neuron is utilized the network output can take on any value. When the final feedforward process is finished, the net compares the neuron outputs to the associative target vectors. The comparative analysis is finished once the net backward-feeds the adjusted weights and biases (backpropagates) to the first layer. Next is a portion of the MATLAB AFCM program that contains the transfer functions.

```
% =====
% Initialize Weights and Biases
% INITFF is used to initialize the weights and biases for
% the three layer (TANSIG/PURELIN) network.
% =====

[w11,b11,w21,b21] = initff(P,S1,'tansig',T1,'purelin')
```

Learning Rule (Hagan *et al.* 1996)

The LMBP approximation, is the learning rule used in this research. This is because of conventional BP is not fast enough and or effective enough to handle the amount of inputs implemented into the model. The LMBP can be thought of as an enhanced BP because it uses a technique from BP, a gradient descent method, plus the Gauss-Newton method. The combination of these techniques allow the neural network to train with a high degree of efficiency. While the Gauss-Newton method usually produces faster convergence than steepest descent, the behavior of this method can be quite complex and not always used by the LMBP algorithm. When this algorithm senses any sort of divergence to locating minimum mean square error it utilizes the steepest descent

steps, putting the Gauss-Newton method on standby. A problem with the Gauss-Newton method is that it requires the computation and storage of the Hessian matrix, as well as the inverse. Steepest descent is guaranteed to converge, if the learning rate is not too large or if we perform a linear minimization at each stage. A positive aspect to the Gauss-Newton method is that it does not require calculation of second weight and bias derivatives.

While training the model, the variation between these two techniques can be witnessed by the Levenberg-Marquardt parameter, μ . As the program runs, the training process is depicted on the screen of the monitor that can be set to the designers preference (df). Along with a maximum number of epochs to train to (me) and a sum-squared error goal (eg).

```
df = 2; % Frequency of progress displays (in epochs).
me = 1000; % Maximum number of epochs to train.
eg = 0.015; % Sum-squared error goal.
```

The training is made possible by the programming below:

```
% =====
% TRAINLM - Trains a feed-forward network with faster bckprp.
% Training the Neural with a Levenberg-Marquardt Backpropagation Algorithm
% =====

tp = [df me eg],

[w11,b11,w21,b21,w31,b31,ep,tr]=
trainlm(w11,b11,'tansig',w21,b21,'tansig',w31,b31,'purelin',P,T1,tp),
```

where the training parameters (tp) dictate the neural net/user relationship, epoch (ep) is the presentation of the set of training (input and/or target) vectors to a network and the

calculation of new weights and biases, and **trainlm** initializes the Levenberg-Marquardt training procedure.

The association of the target vectors and the output vectors of the neural net are made by invoking the input vectors through the adjusted neural net. This is done by the following programming,

```
% =====  
% Trained Fuel Consumption  
% SIMUFF - Simulates a feed-forward network.  
% =====  
  
TWf= simuff(P,w11,b11,'tansig',w21,b21,'purelin')*U.
```

The neural net is now trained to predict the point fuel consumption. The trained fuel consumption (TWf) should be able to map the original fuel consumption data generated by the AFBM. The comparative analysis of the trained vs. the actual data should have values within 3% of the original. This should not be confused with the sum-square error that the net was given as a training threshold. The formulation of the input vectors allow the user to change P (input) to any specific velocity and altitude, giving the corresponding neuron output, fuel consumption. In order to satisfy the objective, which states “develop a flexible, computationally efficient, and accurate aircraft fuel consumption model”, the following investigation is required. Testing the neural net with randomly generated inputs and have that data compared to the fuel flow that is calculated by the AFBM using the randomly generated data (GAFBM) from the net. If the neural net is working correctly the comparison of these data sets should be very similar, within $\pm 3\%$ is a likely value. As stated above, this can be deceiving to a first time user who believes the sum-square error goal is what decides on the true difference between each corresponding data set.

The AFCM model is “flexible” because the user can manipulate the program code to accept all types of aircraft. Another addition to the models flexibility is the way in

which the user can use different transfer functions when appropriate, alter the sum-square error goal so that it trains to a lower or higher threshold, and even the change the architecture of the whole model. This can all be done by editing the MATLAB neural net code at the press of a finger.

4.3 *Statistics of Performance Data*

Statistical procedures are used in this research to compare one procedure against another: the collection and the analysis of data in the presence of variability. Several statistical methods will be used to assist in making inferences about the above processes on the basis of imperfect data.

4.3.1 *Statistical Methods* (Hogg *et al.*, 1992)

- Mean - arithmetic average of a sample number of observations, n . In this case the number of observations are six-hundred unique fuel consumption's (Wf). For the given Wf data set x_1, x_2, \dots, x_n multiplied by the inverse of n observations, we can denote it by

$$\bar{x} = \frac{1}{n}(x_1 + x_2 + \dots + x_n) = \frac{1}{n} \sum_{i=1}^n x_i .$$

Note that the deviations of the observations from the mean, $x_i - \bar{X}$, $i = 1, 2, \dots, n$, always add to zero; that is,

$$\sum_{i=1}^n (x_i - \bar{x}) = \sum_{i=1}^n x_i - n\bar{x} = \sum_{i=1}^n x_i - \sum_{i=1}^n x_i = 0 .$$

One can think of the mean as the fulcrum point that keeps a weightless ruler, on which each observation is represented by the same weight, in perfect balance.

If we consider six-hundred Wf's, then

$$\bar{x} = \frac{1}{600} \sum_{i=1}^n x_i$$

For the complete set of six-hundred data points, the average or mean is \bar{x} . One problem with the mean as the center of a data set is that it is effected by the presence of one or several data points that lie very far to one side of the other values. This is called an outlier. The AFCM was designed to eliminate these types of outliers by constraining the velocity to certain altitudes. For example, FAA requires all commercial aircraft to travel at speeds less then 250 knots when at an altitude of 10,000 feet or less. Applying this rule to the program eliminated data that would normally not comply with the FAA rule. There is still ambiguity within the data set in the high range, where an aircraft can fly at 200 knots with at an altitude of 45,000 feet: this is not realistic for level flight.

Measures of Variation

The standard deviation and variance are common measures of variability. The sample variance and its square root, the standard deviation are measures of spread that are based on normally distributed samples. The variance is the minimum variance unbiased estimator of the normal parameter σ^2 . The standard deviation has the desirable property of being in the same units as the data. That is, if the data is in lb/hr the standard deviation is in lb/hr. The variance is in $(\text{lb/hr})^2$, which is more difficult to interpret. Neither the standard deviation nor the variance is robust to outliers. A data value that is separate from the body of the data can increase the value of the statistics by an arbitrarily large amount.

- Variance-the square $(x - \bar{x})^2$ of the distance $|x - \bar{x}|$ of an observation x_i from the overall average \bar{x} provides some information about the variability, $i = 1, 2, \dots, n$. The variance is a special average of these n squared distances and is defined as

$$s^2 = \frac{1}{n-1} [(x_1 - \bar{x})^2 + (x_2 - \bar{x})^2 + \dots + (x_n - \bar{x})^2] = \frac{1}{n-1} \sum_{i=1}^n (x_i - \bar{x})^2 .$$

As stated above, it is the average of n such components, but we have divided the sum by $(n - 1)$ instead of n . This is because it was noted that the n deviations $(x_i - \bar{x})^2$, $i = 1, \dots, n$, add up to zero. Hence, we really need only $(n - 1)$ of these deviations to calculate s^2 . It is always possible to obtain the last deviation from

$$(x_n - \bar{x}) = - \sum_{i=1}^{n-1} (x_i - \bar{x}) .$$

Therefore it seems justifiable to divide by $n - 1$ instead of n . The difference between the two denominators make very little difference to large data sets (Schiff, 1996). An easier way of calculating the variance that avoids working out the deviations from the mean is

$$s^2 = \frac{1}{n-1} \left[\sum_{i=1}^n x_i^2 - \frac{\sum_{i=1}^n (x_i - \bar{x})^2}{n} \right] .$$

- Standard Deviation-otherwise known as the Root Mean Square is simply the square root of the variance. This method returns the original units of measurement and denoted as

$$s = \sqrt{s^2} = \sqrt{\frac{1}{n-1} \sum_{i=1}^n (x_i - \bar{x})^2}$$

- t-test-is used in comparing two means, its purpose being to tell whether the means of two sets of data are significantly different. The probability level corresponds to computed **t** is the probability that the two means are truly different. In testing the significance of means, the conventional procedure is to declare the difference significant at the 95% probability level and highly significant at the 99% level. The t-test consists of testing the truth of a hypothesis that two means are the same. This is called the *null hypothesis*. The procedure is to calculate the probability of finding a difference on the assumption that the null hypothesis is true. If the probability is sufficiently small, the null hypothesis is rejected and we conclude that the two means are truly different.

Conditions of the *null hypothesis*

Do **not** Reject if **H₀**: $\mu_1 = \mu_2$ Reject if **H₁**: $\mu_1 \neq \mu_2$

For this test it will be assumed that the standard deviation, σ , is the same for both means, because average fuel consumption was similar in both tests. The null hypothesis to be tested is that the AFCM (X) and the AFBM (Y) are not significantly different. The following method for calculating **t** was used in the research:

$$\bar{W}/(S_w/\sqrt{n}) \geq t(\alpha; n - 1).$$

This is called a paired-sample t-test where, \bar{W} is the difference of each paired data set (X, Y), S_w is the sample variance of the differences, and n is the number in the sample set. The fuel consumption data was calculated on the basis that the input data set of the AFBM (X) came from the AFCM (Y), and was expected to generate the same fuel consumption's. In this case the X_i and Y_i are independent but expected to be related. In such a situation we analyze the differences, $W_i = X_i - Y_i$ because these differences “cancel” or adjust for subject differences that make measurements X and Y both appear usually high or low. The differences $W_1 = X_1 - Y_1$, $W_2 = X_2 - Y_2$, ..., $W_n = X_n - Y_n$ are

then a random set of size n from a normal distribution with estimated population means $\mu_1 - \mu_2$ and variance σ^2_w . The random variables W_1, \dots, W_n are independent because they are from observations on different sets of data. The distribution of W is normal, hence we can use the t-test statistic. The summary of results for the aircraft set is depicted in Table 2.

4.4 Output of the Model

The output is the information provided by the AFCM. With the help of statistics and graphics we can see how well the neural net trains and graphs the output of the model. The output allows the user to make judgment on the data set and the functionality of the model.

The individual models, AFBM and NNOM can be probed for information as well. The AFBM is the bench mark for the entire research, without the output from this model the AFCM would not exist. A t-test will be run for each pair of data that is generated by these two models. If the results prove to be acceptable or we can accept the null hypothesis then the models functionality is effective. All the statistical analysis is done in MINITAB (Version 10Xtra, © Minitab, Inc., 1995).

5. MODEL APPLICATION AND ANALYSIS

5.1 *Introduction*

This chapter presents the application of the developed AFCM. The model has been tested with several different neural net architectures, two and three layer neural nets accepting a range of input data that started at 225 randomly generated velocities and altitudes. Each velocity had its own corresponding altitude. The AFCM used this data to generate the fuel flow that was utilized as the target vector for the neural net. Other data sets were tested, and it was decided to use 600 randomly generated sets. The results of this research will contain graphical representation and statistical analysis of the data. A Boeing 747-100, Boeing 767-200, Bombardier Dash-7, DC10-30 and Jetstar were used for the performance calculations to show the strength and validity of the AFCM. The Boeing 747-100 was used as the initial test aircraft for this research. It is widely known around the world and can be termed “the power-house” of commercial aviation transports. The aircraft, developed by Boeing in the mid-1960’ is primarily a trans-oceanic aircraft. Its massive fuselage and fuel capacity can hold approximately 450 passengers traveling at stage lengths of nearly 5,000 miles. This is made possible by the maximum take-off weight to fuel ratio of 3:1.

5.2 *Model Application*

The AFCM can be applied to future research in the aircraft fuel consumption modeling arena. This research provides the “stepping stone” for future models that can test any aircraft’s fuelburn under multiple variations of the airframe and the attitude at which it flies. For example, an enhanced AFCM can handle multiple input variables such as flap settings, gear position, weight change, and the attitude or position in which the aircraft is flying: banking, G forces, etc.. The current model can produce fuel

consumption, thrust, velocity (both in Mach # and knots), altitude, and atmospheric parameters at any point within the aircraft's flight path.

5.3 *Model Input Parameters*

To demonstrate the versatility of the AFCM, the following data for each aircraft can be manipulated. The Boeing 747-100 data is shown below and the rest of the aircraft mix can be found in Appendix A.

Aircraft Characteristics

<u>Aircraft</u>	B747-100	Engine	JT9D-3A
	VNE (not exceeding) = 517.00 knots		VS = 110.00 knots
	Operating Empty Weight		
	Maximum Takeoff Weight = 740,000 lb.		
	Number of Engines = 4		Wing Area = 5,500.00 ft ²

AFBM Envelope: Velocity 200 knots - 300 knots (IAS)
Altitude Sea Level (0 ft) - 45,000 ft.

Random Generator: 600 data points between the above envelopes.

Altitude Sensitivity: Troposphere (0 - 36,089 ft.) & Stratosphere (36,089 - 45,000 ft.)

ρ = air density [lb/ft³]

σ = atmospheric density ratio

δ = pressure ratio

sv = sonic velocity [knots]

The AFCM calculates these parameters to simulate a dynamic atmospheric environment. When calculating Mach number the above parameters are utilized to give variations of speed as a function of altitude. The following MATLAB programming calculates the Mach number:

$$M(i) = \text{sqrt}(5 * [(r(i) * ((1 + 0.2 * [v(i)/661.5]^2)^{3.5} - 1) + 1)^{0.286} - 1]),$$

where r is the inverse of the pressure ratio, δ , and v is the IAS. Figure 8 represents the core equation constants that were extracted from SIMMOD, and found in the program directory:

SIM\PROVER\PROGS\

Core Equation Constants for Boeing 747-100:

C(1) = 0.21105264	K(1) = 0.0151073814
C(2) = 0.263755463	K(2) = -1.10763705E-06
C(3) = -0.16161515	K(3) = 4.49822265E-08
C(4) = 0.0758395116	K(4) = 0.0542092256
C(5) = 0.0249066916	K(5) = -0.00853030039
C(6) = -0.0253689568	K(6) = 0.00113895091
C(7) = 0.149698643	K(7) = -6.32908055E-05
C(8) = 0.493944407	K(8) = 1.28082643E-06
C(9) = 0.0738636868	K(9) = -0.00092774075
C(10) = -0.223604847	K(10) = 0.0195524624
C(11) = -0.00700041482	K(11) = -0.00217159804
C(12) = 0.0328436526	K(12) = 8.49267355E-05
C(13) = 0.0435177226	
C(14) = 0.00514188666	
C(15) = 0.00134403024	
C(16) = 0.0306193895	
C(17) = 0.00983454066	
C(18) = -0.00845369234	

FIGURE 8: Partial Aircraft Echo Report

The other core equation constants are also in Appendix A.

Change of Velocity Units: along with functions of fuel flow, thrust, lift coefficient and drag coefficient, velocity units must be in feet/second rather than knots. The following equation converts the velocity to ft/s by

$$V(i) = M(i)*sv(i)*1.6867,$$

where the product of Mach number and Sonic Velocity has units of knots that is multiplied by the conversion factor of 1.6867 to give ft/sec.

The AFBM computes all the above to generate the fuel flow of that specific aircraft. MATLAB allows the user to count floating point operations. The AFCM, as well as the submodels have independent flop counters. Table 2 represents the results of the models computational intensity [flops].

TABLE 2: Floating Point Operations

Model	Function	Technique	No. of Layer's Per Network	No. of Neuron's Per Layer	Flops
AFBM	Energy Balance	Polynomial	-	-	89,600
AFCM2_6	TRAINLM	LMBP	2	6	Rarely Converged
AFCM2_7	TRAINLM	LMBP	2	7	56,400
AFCM2_8	TRAINLM	LMBP	2	8	64,200
AFCM2_10	TRAINLM	LMBP	2	10	79,800
AFCM3_6	TRAINLM	LMBP	3	6	117,000
AFCM3_8	TRAINLM	LMBP	3	8	125,800

Computationally, the AFCM has satisfied the objective by illustrating that the AFCM2_7 was less computationally intensive. It was found that testing of various neural net architectures the two-layer, seven-neuron model was **38%** more efficient than Collins path performance AFBM. Further results are still needed to totally satisfy the objective. These will be presented in the next section.

5.4 Model Results

Now that the AFCM level of performance is determined, and proving its performance to be faster than the AFBM, we can move on to the next portion of the results that determine the functionality and accuracy of the model.

First, to insure that the AFBM is running correctly we can look at all the pertinent output that reflects on the functionality of the model and most importantly the fuel consumption profile of the model. This profile along with the velocity and altitude will be the key part of the AFCM.

5.4.1 Graphical Analysis

Boeing 747-100 data will be used as for the graphical representation

FIGURE: 9

The plot of Velocity vs. Altitude illustrates the difference in velocity [TAS] as the atmosphere changes. The profiles points are used as input vectors for the AFCM, initially the AFBM utilizes the two variables to calculate fuel consumption. Once the fuel consumption is calculated, inputs (velocity, altitude) and target vectors (fuel consumption) funnel into the neural network.

FIGURE: 10

The graph illustrates the AFBM fuel consumption as a function of velocity and altitude. The plot depicts the aircraft velocity and altitude limitations. For example the Boeing 747-100 will travel at speeds of ± 300 knots with a ceiling of 45,000 feet, where as the Bombardier Dash-7 will not exceed 230 knots and 20,000 feet of altitude.

FIGURE: 11

The graph illustrates the drag vs Mach number and lift over drag vs Mach number. What the first graph tells us is that drag increase as the aircraft's speed increases. There is a point in every profile where the drag is at the minimum. This is a good point to recognize if fuel efficiency is to be maintained. The second graph shows that lift increases relative to drag when speed is increased. As speed increases with altitude so does drag, hence the ratio of lift over drag decreases.

FIGURE: 12

The plot of M_a vs Mach number, is observed to behave as profile drag. This value generally constant until critical Mach is reached , after which there is an increase. M_b vs Mach number, is observed to behave induced drag, where the value gradually decreases to a minimum point which reflects the wing's most efficient point, after which there is an increase, and more of an increase as critical Mach becomes dominant. M_c vs Mach number behaves much like the induced characteristics, there is a gradual increase until critical Mach effects again cause rapid increase.

As we can see from these graphs, the drag rise associated with critical Mach has a large impact on the shape of the curve.

FIGURE: 13

The first plot illustrates a comparison of fuel consumption's between the trained vs the generalized fuel consumption. Collins model generates the input needed by the NNOM in order to train the weights and biases of the net that help produce the association of input vectors to target vectors. After the network trains to a sum squared error goal (SSEG) of 0.5%, the outputs will compare to the target vectors. Figure 16 represents the statistical results of the trained data to the actual data (Collins). It is important not to associate the SSEG with the difference in the true means of the data set; where the true means can be as large as 4% different. The second plot illustrates the generalized neural net compared to the generalized AFBM (GAFBM).

FIGURE: 14

The plot of the AFCM vs GAFBM is observed to have a relative close correspondence to one another. It tells us that the neural net is generalizing the data of the trained net correctly by comparing it to the AFBM whose inputs are the generalized random output of the AFCM. This tests both data sets for similarity of one another. The next plot illustrates a histogram that represent the combination of the AFCM and GAFBM data. The conclusion we can make from the histogram is that there is a relative similarity between the data sets.

FIGURE: 15

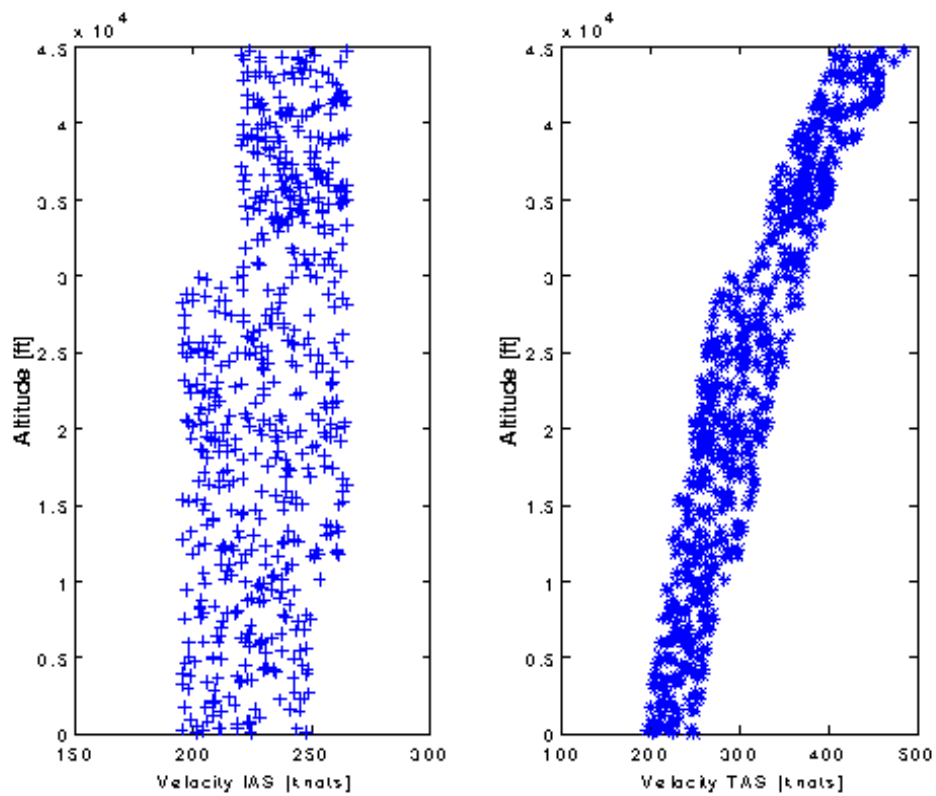
The graph depicts a comparison of a specific input used in both the AFCM and AFBM. A comparison of the fuel consumption output for the models are within 3% of each other.

Figures 9 - 15 denote the Boeing 747-100.



BOEING 747-100

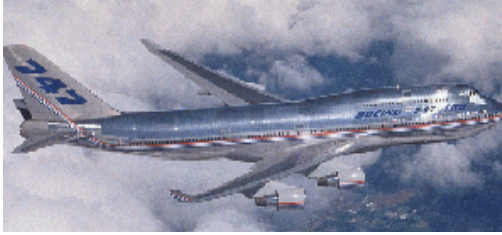
Altitude and Velocity Profiles of IAS and TAS



Legend

+ = Velocity [IAS]
* = Velocity [TAS]

FIGURE 9: Velocity and Altitude Profiles



BOEING 747-100

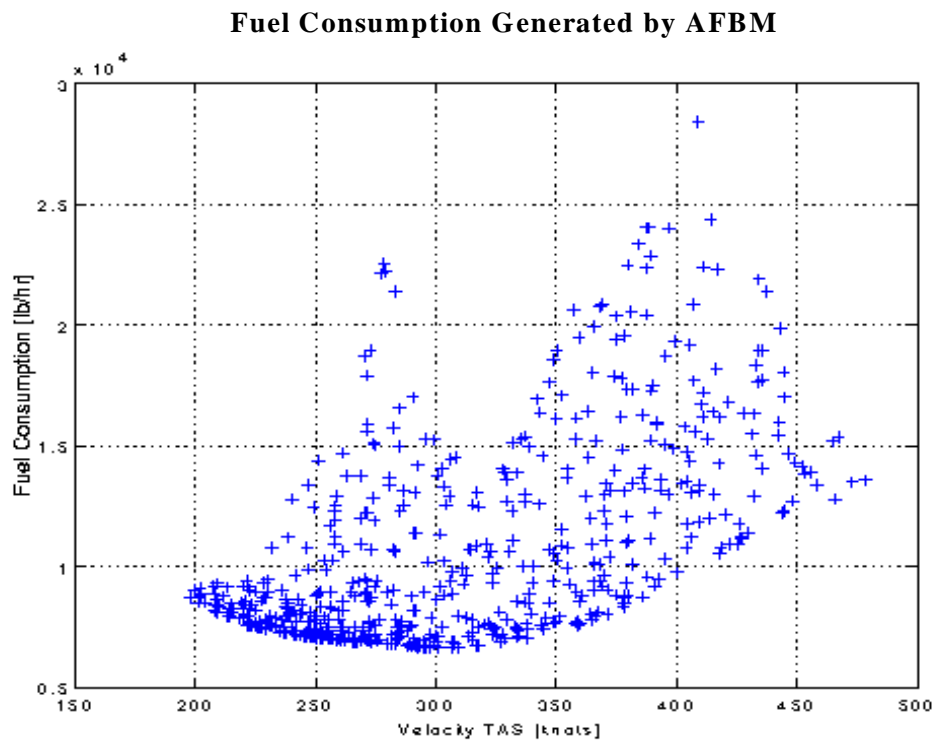
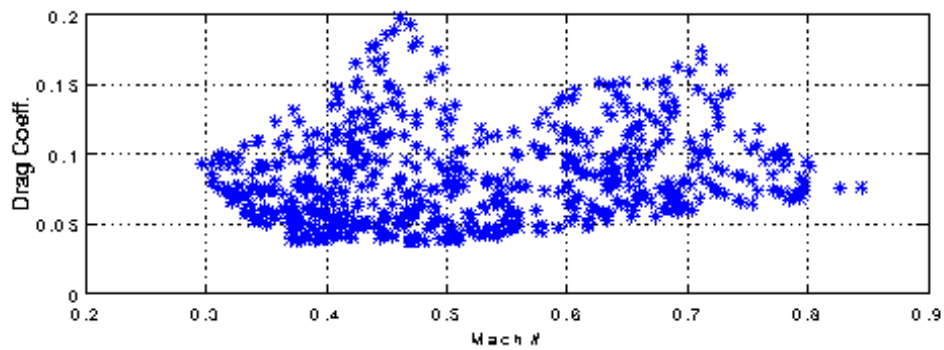


FIGURE 10: Fuel Consumption Before Network Training



BOEING 747-100

Drag Coefficient vs Mach Number



Lift over Drag Ratio vs Mach Number

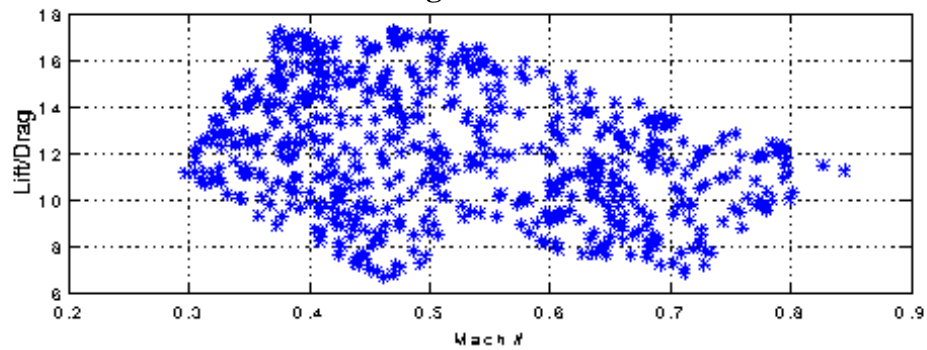


FIGURE 11: Lift and Drag Relationships vs Mach Number



BOEING 747-100

Mach Functions vs Mach Number

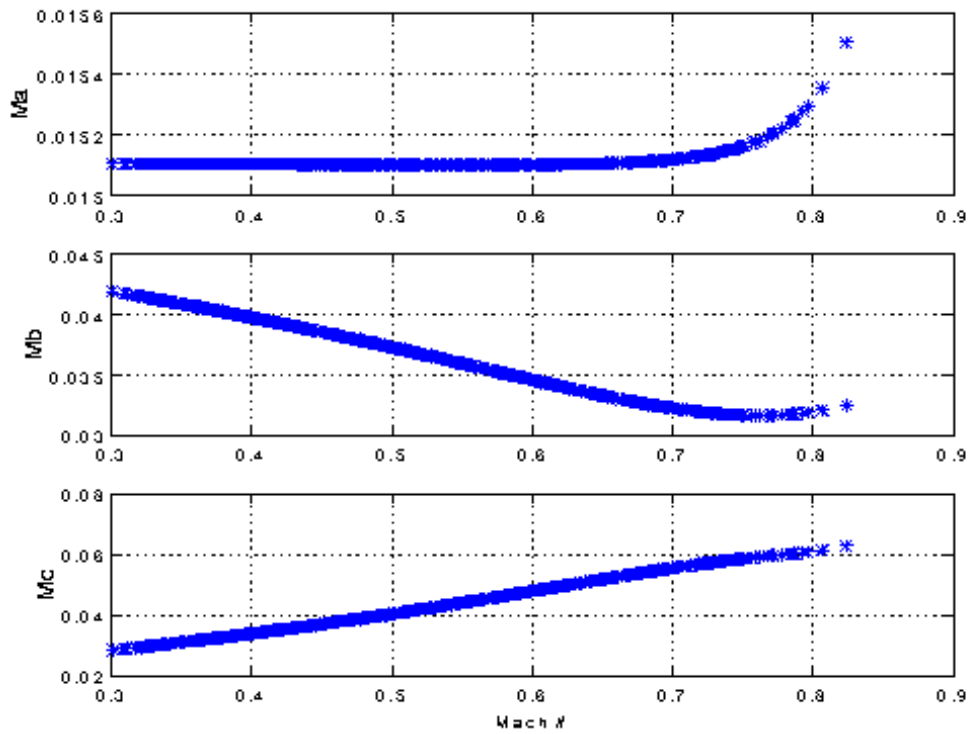
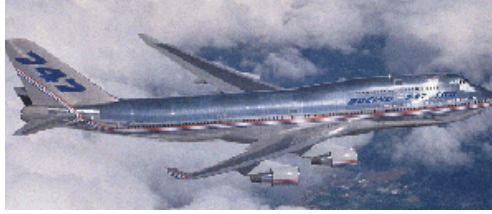
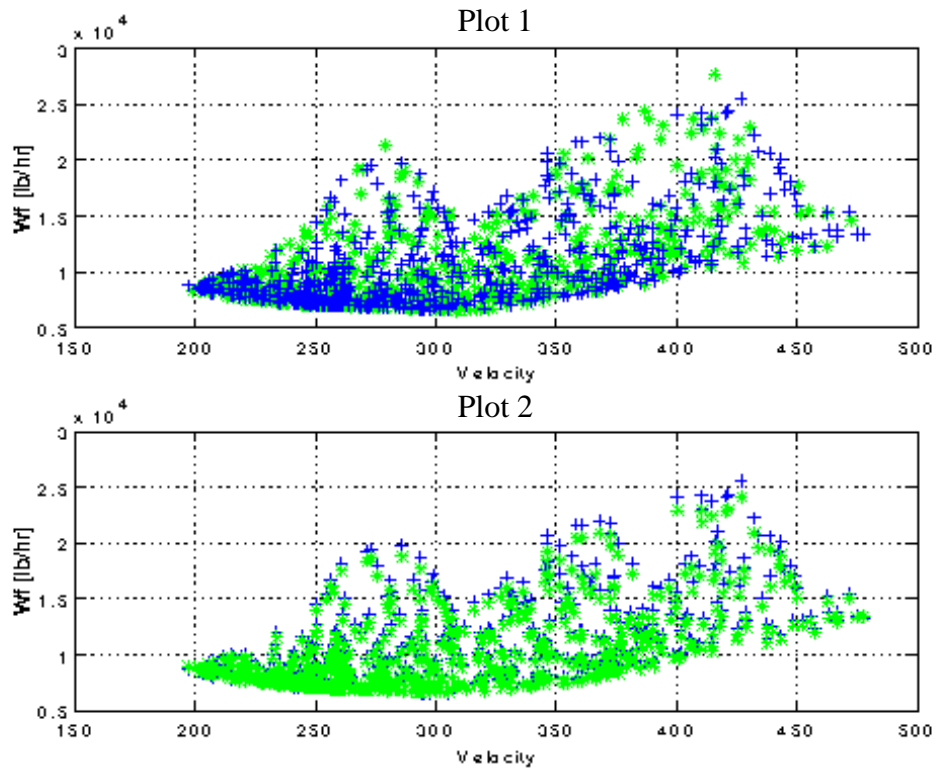


FIGURE 12: Mach Functions vs Mach Number



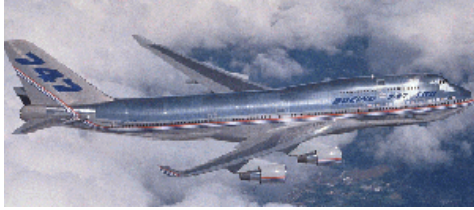
BOEING 747-100

Trained and Generalized Fuel Consumption's



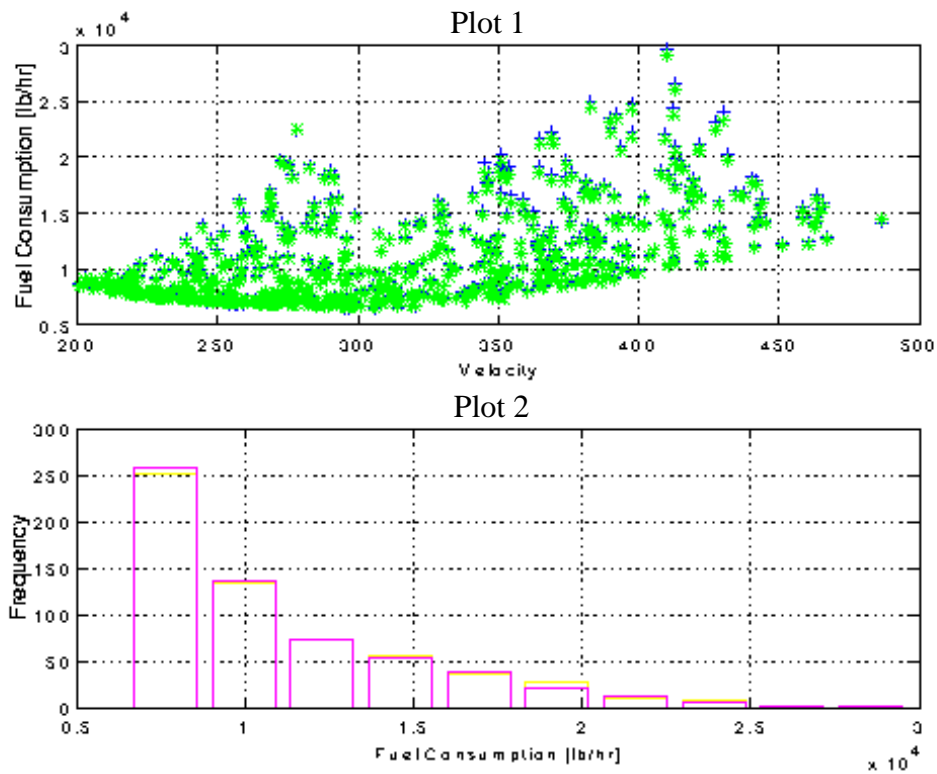
<u>Legend Plot 1</u>	<u>Plot 2</u>
+ = Generalized Neural Net	+ = Generalized Neural Net
* = Trained Neural Net	* = + = Generalized AFBM

FIGURE 13: Trained vs Actual Fuel Consumption and Generalized vs Trained Fuel Consumption



BOEING 747-100

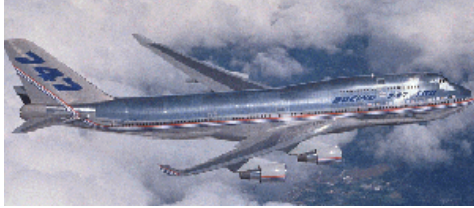
Generalized Compared to Generalized AFBM



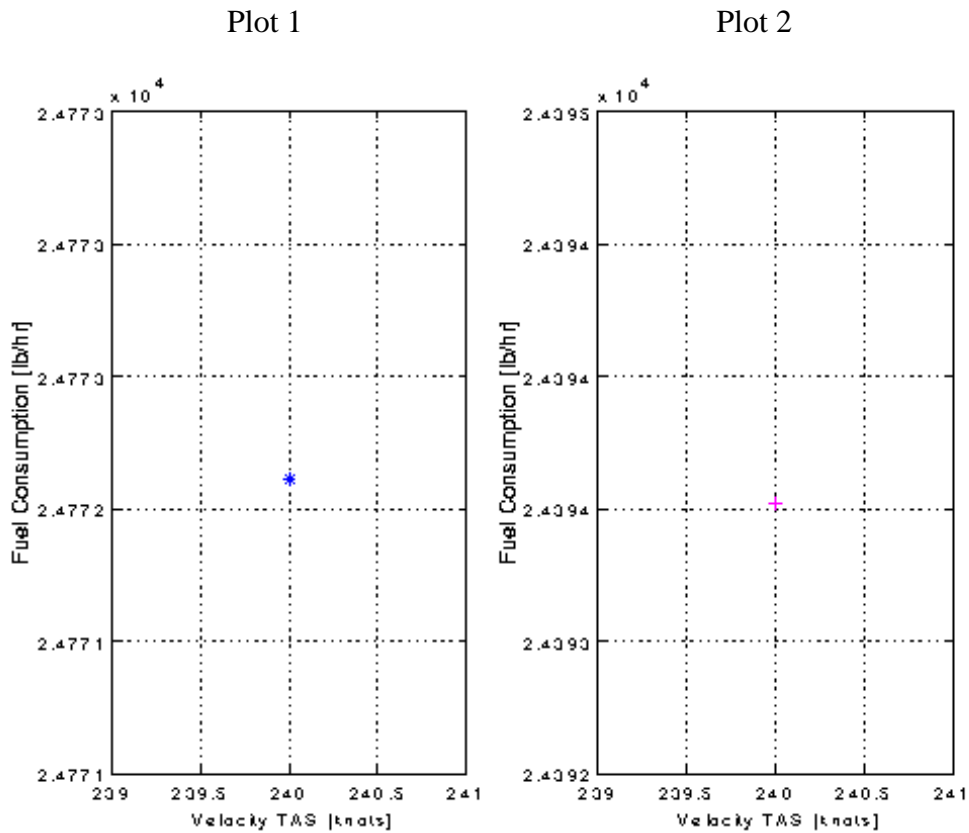
Histogram of the Differences in Fuel Consumption

<u>Legend Plot 1</u>	<u>Plot 2</u>
+ = Generalized Neural Net	Magenta = Generalized Neural Net
* = Generalized AFBM	Yellow = Generalized AFBM

FIGURE 14: Comparison of Fuel Consumption Data



BOEING 747-100



<u>Legend Plot 1</u>	<u>Plot 2</u>
+ = Generalized Neural Net	Blue = Generalized Neural Net
* = Generalized AFBM	Magenta = Generalized AFBM

FIGURE 15: Comparison of Specific Input Fuel Consumption Data

5.4.2 *Statistical Analysis*

The statistical analysis begins with Figure 16: Summary of AFBM-NNOM Statistical Results. The models run well, allowing for all the t-tests to be accepted at the 99% significance level.

Summary of AFBM - NNOM Statistical Results

Aircraft Type	Mean	StDev.	SE Mean	t	t(0.01,599)	P-Value	Reject	Accept
Boeing 747-100	3.97	77.76	3.18	1.25	2.33	0.21		X
Boeing 767-200	0.61	22.20	0.91	0.67	2.33	0.50		X
Dash-7	0.01	1.68	0.06	0.17	2.33	0.87		X
DC-10	2.23	34.10	1.39	1.60	2.33	0.11		X
Jet Star	-0.01	3.16	0.13	-0.11	2.33	0.91		X

FIGURE 16: Summary of AFBM-NNOM Statistical Results

The t-test proves that the NNOM output is not significantly different from the base model, and the functionality of the models are worthy. We can conduct tests of hypotheses by rejecting the null hypothesis, $H_0: \mu_1 = \mu_2$ in favor of $H_1: \mu_1 \geq \mu_2$ if $t \geq t(\alpha; n - 1)$.

Conclusion of the results: the p-value is $> \alpha = 0.01$. Hence, at the 1% significance level we cannot conclude that the trained and actual average fuel consumption's are the not the same for all the aircraft studied. For example, the probability of a difference in the means as extreme as 1.25 (747-100 observation) or greater is a 1 in 20 chance.

The results of the AFCM and AFBM are summarized in Figure 22. The t-test analysis concludes that the generalized data of the neural net when implemented and

compared to the AFBM, that they do significantly differ. The next section will provide the logic behind this test and prove that this data is statistically different but not practically different by means of a confidence interval test (t-interval).

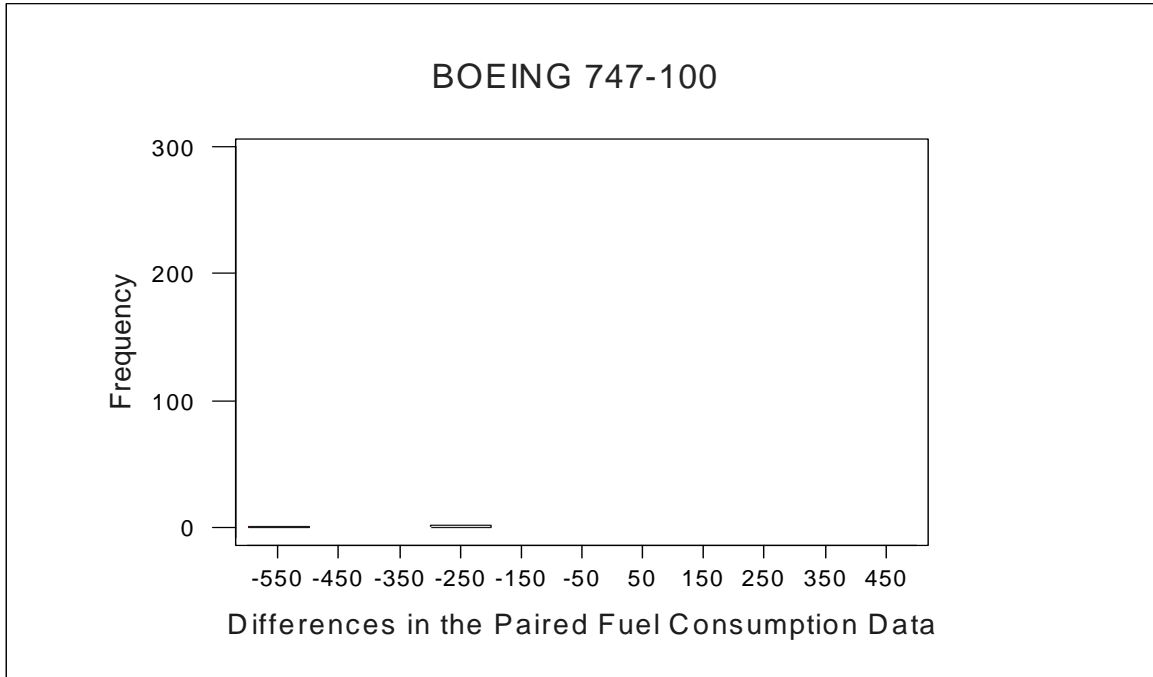


FIGURE 17: Fuel Consumption Differences of a Boeing 747-100

T-Test of the Mean

Null Hypothesis Condition: Test of $\mu = 0.0$ vs $\mu \text{ not } = 0.0$

Aircraft	N	Mean	StDev	SE Mean	t	t ₉₉	P-Value
Boeing 747-100	600	23.97	76.25	3.11	7.70	2.326	0.0000

The t-test computes the differences in the means, where the p-value is the confidence level at which the data is indeed statistically different. Hence, the p-value of **0.0000** means that it is highly probable (99.9999%) that the mean or average of the fuel consumption's are different and that they do not equal each other. The t-value is **7.70** which is significantly larger than the comparative textbook table value $t(0.01;599)$ of

2.326. It is important to understand that this is a statistical difference, and not a practical difference because there is ambiguity within the results. Figure 16 tells us that there is a difference between the data sets but a relatively small difference when comparing each set of fuel consumption data. In general, the most critical area of difference lies within the 50 lb/hr range. Also, the test states that the null hypothesis must be rejected because it does not satisfy the mean conditionally: reject $H_0: \mu_1 = \mu_2$ in favor of $H_1: \mu_1 \neq \mu_2$. It is believed that the larger the sample set the more “power” it has to reject the null hypothesis. This is because a large data set makes it more likely to contain several different ranges of data and outliers. Hence, we can conclude that the means of each set will have a better probability of not being equal to one another.

Confidence Intervals

Aircraft	N	Mean	StDev	SE Mean	99.0 % C.I.
Boeing 747-100	600	23.97	76.25	3.11	(15.93, 32.02)

The C.I. interval computes the hypothetical population mean difference of the paired data set explaining how much the difference of each of these sets are on average. This is a practical statistical approach where as the t-test only depicts statistical information through the null hypothesis. The C.I. interval for this research computed a 99% confidence level that the true fuel consumption means lie within **(15.93 lb/hr, 32.02 lb/hr)**. Using this test proves that the initial assumption is correct: the data sets are closely related. At this point a statistician can not conclude that the C.I. results are within a tolerable fuel consumption range. This is an engineers decision on whether or not the above range is acceptable. The outcome for the results are as follows:

- ◆ 99% of the time the model will produce a true average difference of fuel consumption that lies within a tolerable range.
- ◆ The results are reasonable because **15.93 lb/hr - 32.02 lb/hr** range is considered negligible when assuming an aircraft of this stature burns a minimum of 30,000 lb/hr.

Figures 18-21 will denote the fuel consumption differences and statistical analysis for the rest of the aircraft mix used in this research.

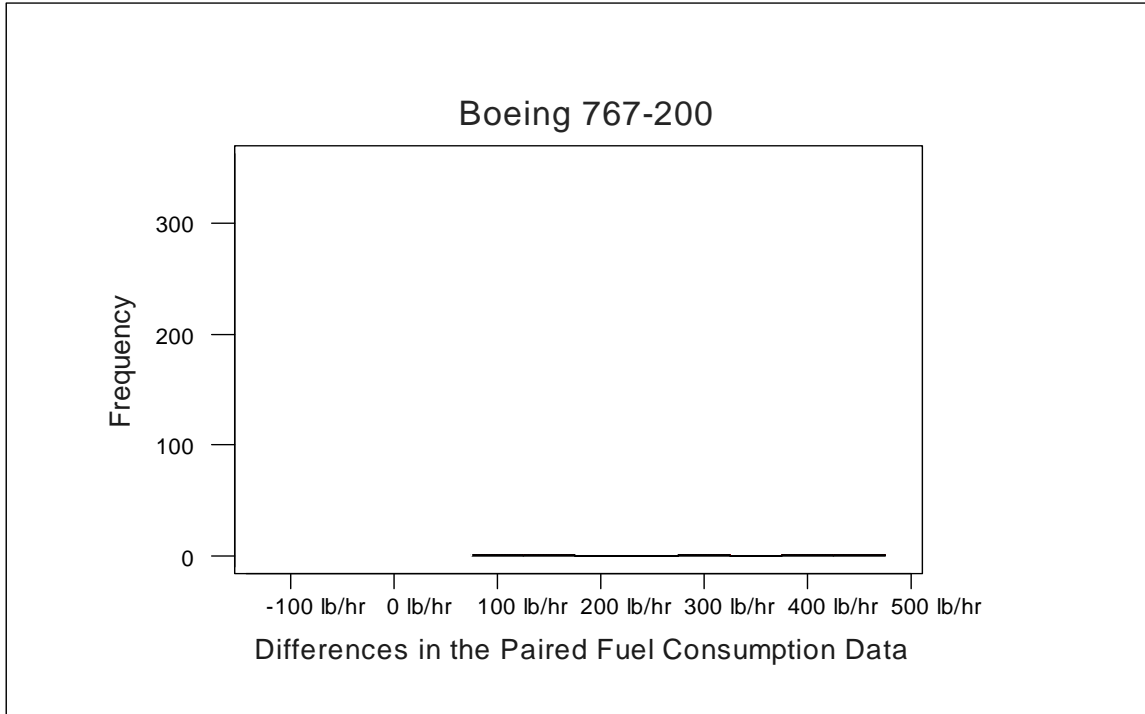


FIGURE 18: Fuel Consumption Differences of a Boeing 767-200

T-Test of the Mean

Null Hypothesis Condition: Test of $\mu = 0.0$ vs $\mu \text{ not } = 0.0$

Aircraft	N	Mean	StDev	SE Mean	t	t ₉₉	P-Value
Boeing 767-200	600	0.95	37.79	1.54	0.63	2.326	0.5400

Confidence Intervals

Aircraft	N	Mean	StDev	SE Mean	99.0 % C.I.
Boeing 767-200	600	0.95	37.79	1.64	(4.9, 13.3)

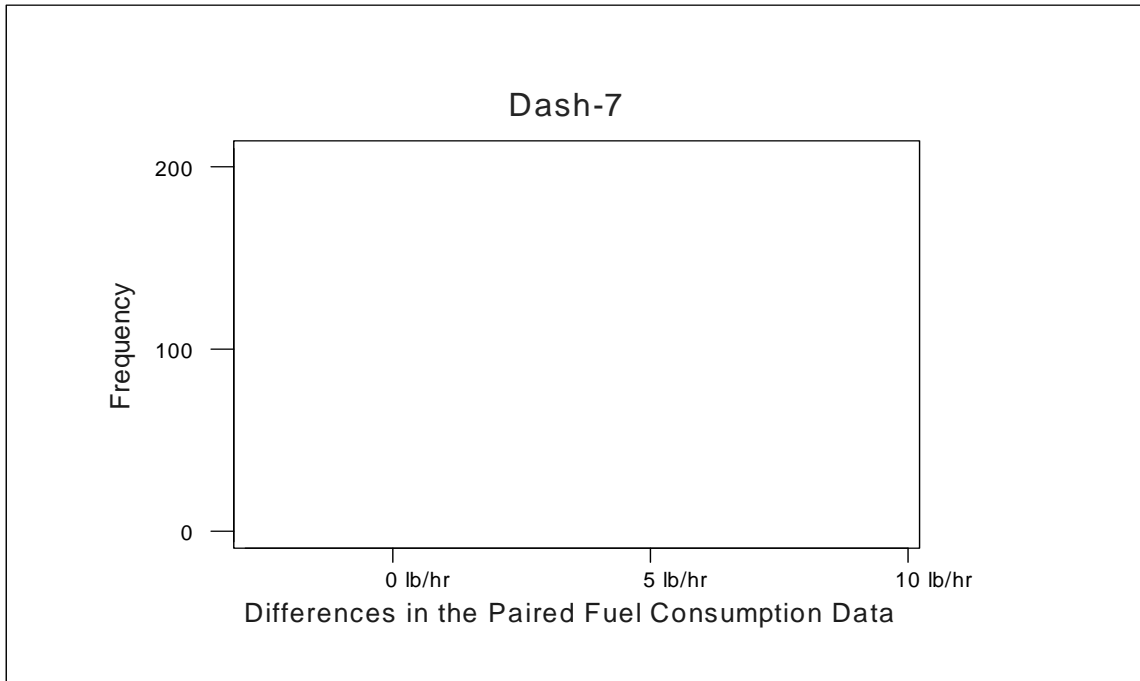


FIGURE 19: Fuel Consumption Differences of a Dash-7

T-Test of the Mean

Null Hypothesis Condition: Test of $\mu = 0.0$ vs $\mu \text{ not } = 0.0$

Aircraft	N	Mean	StDev	SE Mean	t	t ₉₉	P-Value
Dash-7	600	1.36	1.46	1.64	5.54	2.326	0.0000

Confidence Intervals

Aircraft	N	Mean	StDev	SE Mean	99.0 % C.I
Dash-7	600	1.36	1.46	0.06	(1.2, 1.5)

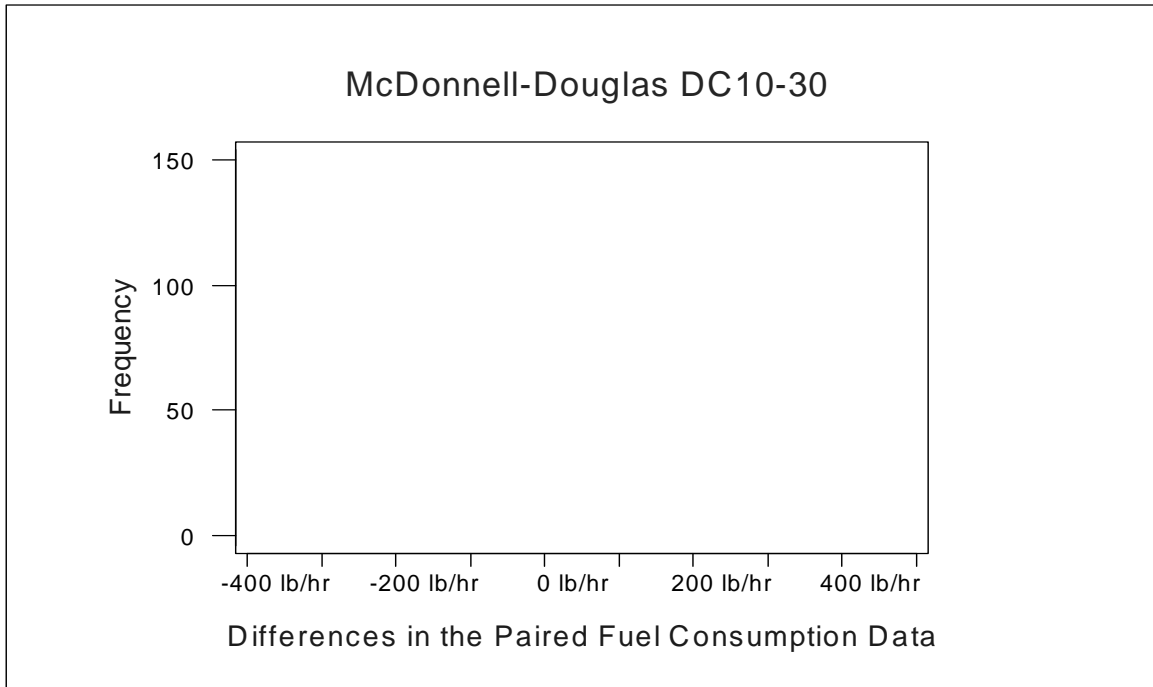


FIGURE 20: Fuel Consumption Differences of a DC10-30

T-Test of the Mean

Null Hypothesis Condition: Test of $\mu = 0.0$ vs $\mu \text{ not } = 0.0$

Aircraft	N	Mean	StDev	SE Mean	t	t ₉₉	P-Value
DC10-30	600	32.80	58.70	2.40	13.71	2.326	0.0000

Confidence Intervals

Aircraft	N	Mean	StDev	SE Mean	99.0 % C.I.
DC10-30	600	32.80	58.70	2.40	(26.7, 39.1)

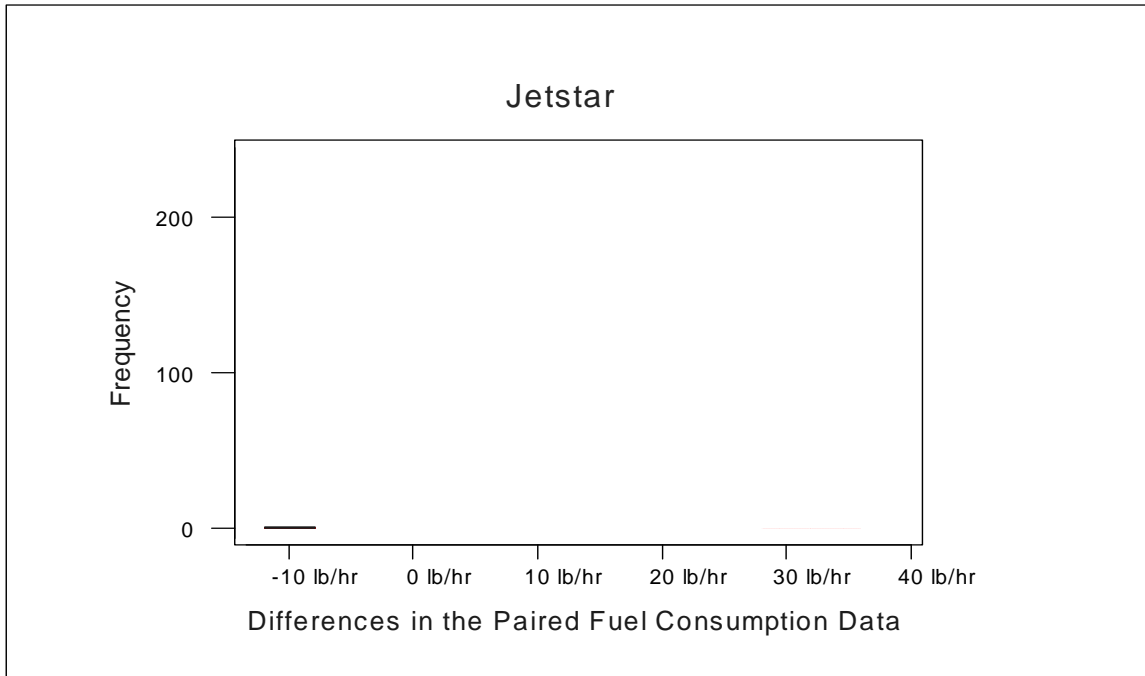


FIGURE 21: Fuel Consumption Differences of a Jetstar

T-Test of the Mean

Null Hypothesis Condition: Test of $\mu = 0.0$ vs $\mu \text{ not } = 0.0$

Aircraft	N	Mean	StDev	SE Mean	t	t ₉₉	P-Value
Jetstar	600	2.05	5.72	0.23	8.80	2.326	0.0000

Confidence Intervals

Aircraft	N	Mean	StDev	SE Mean	99.0 % C.I.
Jetstar	600	2.05	5.72	0.23	(1.45, 2.65)

5.5 Statistical Results

Summary of Statistical Results

Aircraft Type	Mean	StDev.	SE Mean	t	t(0.01,599)	99 % C.I.	P-Value
Boeing 747-100	23.97	76.25	3.11	7.70	2.33	(15.93, 32.02)	0.0000
Boeing 767-200	0.95	37.79	1.54	0.62	2.33	(-3.03, 4.94)	0.5400
Dash-7	1.36	1.46	0.06	22.8	2.33	(1.2, 1.5)	0.0000
DC-10	32.80	58.70	2.40	13.71	2.33	(26.7, 39.1)	0.0000
Jet Star	2.05	5.72	0.23	8.8	2.33	(1.45, 2.65)	0.0000

FIGURE 22: Summary of Statistical Results

The above table concludes that only one out the five aircraft will be accepting the null hypothesis.

Conclusion of the results: the p-value is $> \alpha = 0.01$. Hence, at the 1% significance level we can not conclude that the AFCM and GAFBM average fuel consumption's are the not the same. For example, the probability of a difference in the means as extreme as 0.62 (767-200 observation) or greater is a 1 in 54 chance. The summary of results may be misleading considering only one out the five gives a good t-value. In retrospect, the t-values can be deceptive, the above values are all within a tolerable limit.

6. CONCLUSIONS AND RECOMMENDATIONS

6.1 *Introduction*

This final chapter describes issues underlying the development of the AFCM and the use of the MATLAB Neural Network software. The recommendations are made to improve the accuracy and enhancement of the Aircraft Fuel Consumption Model.

6.2 *Conclusions*

The AFCM developed through this research has been designed to provide air transportation designers the information and foundation needed to encompass an accurate working fuel consumption model into a landside/airside model such as SIMMOD. The objective of this research; to utilize a modeling simulation software to develop a flexible, computationally efficient, and accurate aircraft fuel consumption model, has been accomplished. The energy balance concept in combination with a neural network was successfully developed and applied to modeling aircraft energy performance. The energy balance algorithm accepts as inputs aircraft specific limitations, such as velocity, altitude, and weight. Other equations compensate for altitude change giving both minimum and maximum conditions. When the performance data is generated it directly goes into the neural net as input vectors and target vectors. Two inputs containing 600 randomly generated pieces of data flow feedforward and then are backpropagated until the net reaches its sum-square error goal. These inputs have a direct relation with the target vectors. This relation or association is what makes the neural net so powerful. Once the net has trained it can handle any input with a finite amount of discontinuities and deliver accurate output that is comparable to the AFBM. The beauty about the neural net is that it learns through optimization how to generalize input at a fraction of the computational expense relative to other programs that do the same tasks. Computationally, the AFCM

has satisfied the objective by illustrating that it was indeed less computationally intensive. It was found that through testing various neural net architectures the two-layer, seven-neuron model was **38%** more efficient than Collins path performance AFBM and remain just as accurate.

The level of computational effort of this model could be viewed as “low level” because of the absence of input variables. Typically a fuel consumption model would incorporate many variables. The two input variables, velocity and altitude satisfy the present research and give light to future model’s that could incorporate many input variables. By using the aircraft’s total energy as point performance rather than path performance the AFCM is an efficient model for computing point performance for a multiple range of aircraft. The computational efficiency makes it attractive for parametric studies as well as enhancement.

It was verified statistically that the AFCM was competent in computing fuel consumption as a point performance model. The trained data set was within $\pm 3\%$ of the actual data, and the generalized data set was within $\pm 4\%$ of the generalized AFBM.

In conclusion, this model is practical for modeling fuel consumption. The SIMMOD fuelburn post-processor utilizes the energy balance concept but lacks in the versatility and thrives on computational expense. At the present time, AVERAGE ERROR - Over the entire three dimensional state, we sample any data point on the average and approximately get $\pm 4\%$ discrepancy of fuel flow. Whereas SIMMOD has a high discrepancy within some of its aircraft mix. For example, if a commercial aviation company such as USAir would like to find out how much their F-28 aircraft uses via SIMMOD, the fuel coefficients for that aircraft are of a DC-9 giving a 25% inaccuracy. This discrepancy is extremely high and this is the reason USAir would never utilize SIMMOD for estimating fuel consumption.

- If a substitution is given for an undefined aircraft which delivers 25% inaccuracies, then why use the fuelburn post-processor in the first place? The fuel burn post processor will hinder the confidence of the outputs. Therefore, redefine the entire aircraft mix to achieve a high level of confidence in the output.

Arguments: If it is tolerable for SIMMOD to have 4% maximum difference between calculated and published values and 1.4% average error, then it is better to apply the tolerable errors to the entire aircraft mix instead of having 17 aircraft in the mix defined while 90 remain undefined. The AFCM can be implemented to take over for the AFBM with near accurate values. In one case the 3% - 4% difference of the AFCM to the AFBM could be the exact value of the published data that Collins based his error differences on.

In addition to the AFCM's use for determining point performance of an aircraft it can be easily used as a dynamic path profile model as well. In order to do so the user can take point performance at two different points within the profile, integrate over that distance with respect to time, and generate path like performance. The next section will be the recommendations to this research.

6.3 Recommendations

The goal of the recommendations are to provide the reader with the sort comings of the model and positive insight to a future model. A highly significant recommendation would be to try this model with multiple inputs such as flap settings, landing gear, and more atmospheric conditions such as head wind. The AFCM is a quasi-steady state model where time has no inference, it would be desirable for the model to become path performance oriented. Also to be able to incorporate banking forces and or gravitational forces under implications that fuel consumption changes drastically with these conditions.

One of the concerns in this research is the way Collins derived the core coefficients. These coefficients are aircraft specific, the question is how they were generated. Considering that the drag coefficient plays a major role in the energy balance equation, it is to my understanding that there are several ways of determining drag coefficients. Another recommendation would be to identify a more precise way in determining drag coefficients or use a three-way methodology where the modeller can take an average of three techniques used in determining drag forces. The following methodology could apply:

- ◆ Use of aeronautical calculations: finding drag coefficients through empirical formulation.
- ◆ Wind tunnel tests, using an aircraft model.
- ◆ Actual full scale aircraft testing.

Typically the above processes are nothing new but if we can refine the way in which this data is collected and take the average values of the three techniques we could better each aircraft specific constants. The question now is

- ◆ How does the empirical formulation compare to the wind tunnel testing?
- ◆ Does the output have a small margin of error?
- ◆ How does the empirical formulation compare to the actual aircraft's data?
- ◆ Do any of the above coincide with one another having a minimum margin of error?

One of the other important factors to expose is that drag coefficients do not have a direct correlation with the internal workings that exist within a turbo jet engine. It is recommended to gather internal engine performance data to see if there is any validity in this concept. To do so, the following is recommended:

- ◆ Gather historical data from engine tests at both airline and engine overhaul shops.
- ◆ Obtain airline in-flight recordings

These are the main recommendations as a result of the exposure and experience gained in developing the AFCM. I further believe these are valid points to test and apply to a future AFCM.

BIBLIOGRAPHY

1. "Aircraft Data." Federal Aviation Administration Advisory Circular 150/5325-5C. FAA, 1987.
2. Antsaklis, P.J., and Moody, J.O. "The Dependence Identification Neural Network Construction Algorithm." *IEEE Transactions on Neural Networks*, Vol. 7, No.1, January 1996, pp. 3-15.
3. Baran, Robert H. and Coughlin, James P. "Neural Computation in Hopfield Networks and Boltzmann Machines." Newark: University of Delaware Press, 1994.
4. Barbeau, E.J. "Polynomials." New York: Springer-Verlag, 1989.
5. Beal, Mark. and Demuth, Howard. "Training Functions in a Neural Network Design Tool." In *Proceedings of the Third Workshop on Neural Networks Academic/ Industrial/ NASA/ Defense '92*. SPIE Vol. 1721, 1992.
6. Burrows, James W. "Fuel Optimal Trajectory Computation." Boeing Computer Services Company. Seattle, Wash. AIAA 82-4084, Vol. 19, No.4, April 1982.
7. Collins, B.P., Bell, Noel. J., and Ford, David. W. "Concepts for Aviation Fuel Efficiency." *Aviation Fuel Consumption Symposium*, September 10-11, 1984.
8. Collins, B.P. "Derivation and Current Capabilities of the Path Profile Fuel Consumption Algorithm." The MITRE Corporation. McLean, VA. MTR-80W195, September 1980a.
9. Collins, B.P. "Estimation of Fuel Consumption of Commercial Jet Aircraft from Path Profile Data." The MITRE Corporation. McLean, VA. MP-80W7, May 1980b.
10. Collins, B.P. "Estimation of Turbojet Fuel Consumption from Tracking Data." The MITRE Corporation. McLean, VA. MTR-79W344, September 1979.
11. Ecker, Joseph G. and Kupferschmid, Michael. "Introduction to Operations Research." New York: John Wiley & Sons, 1988.

12. Ethell, Jeffrey L. "Fuel Economy in Aviation." NASA SP-462, Washington, DC., 1983.
13. Etter, D.M. "Engineering Problem Solving with MATLAB®." NJ: Prentice Hall, Englewood Cliffs, 1993.
14. Gosselin, C.M., Le-Huy, H., and Payeur, P. "Trajectory Prediction for Moving Objects Using Artificial Neural Networks." *IEEE Transactions on Industrial Electronics*. Vol. 42, No.2, April 1995, pp. 147-158.
15. Grossberg, S., "Competitive Learning From Interactive Activation to Adaptive Resonance." *Cognitive Science*, 11, 23-63.
16. Hagan, M., Demuth, H., Beal, M., "Neural Network Design." New York: Thomas Publishing Co., 1996.
17. Hogg, Robert. V., Ledolter, Johannes. "Applied Statistics for Engineers and Physical Scientists." New York, Macmillian Publishing Company, 2ed., 1992.
18. Khanna, T. "Foundations of Neural Networks." New York: Addison-Wesley, 1990.
19. Lau, C., "Neural Networks: theoretical foundation and analysis." New York: IEEE Press, 1992.
20. Mair, Austyn. W., and Birdsall, David. L., "Aircraft Performance." *Cambridge Aerospace Series 5*. New York: Cambridge University Press. 1992.
21. Maren, Alianna J. "A Logical Topology of Neural Networks." In *Proceedings of the Third Workshop on Neural Networks - Academic/ Industrial/ NASA/ Defense '92*. SPIE Vol. 1515, 1991.
22. *MATLAB* ® 4.0 ©. The Math Works Inc., 1992.
23. McCormick, Barnes W. "Aerodynamics, Aeronautics and Flight Mechanics." New York, London: John Wiley & Sons, 1995.
24. *MINITAB* ® 10Xtra ©. Minitab Inc., 1995.
25. Murphy, John H. "Neural Network Learning Algorithms." In *Proceedings of the Third Workshop on Neural Networks - Academic/ Industrial/ NASA/ Defense '91*. SPIE Vol. 1515. 1991.
26. *Neural Network TOOLBOX* 2.0 ©. The Math Works Inc., 1994.

27. Ripley, Brian D. "Networks and Chaos: Statistical and Probabilistic Aspects." eds. O.E. Barndorff-Nielsen, J.L. Jensen, and W.S. Kendall. London: Chapman & Hall, 1993.
28. Roskam, J. "Airplane Design: Part I, Preliminary Sizing of Airplanes." Roskam Aviation and Engineering Corporation. Kansas: Ottawa, 1989a.
29. Roskam, J. "Airplane Design: Part II, Preliminary Configuration Design and Integration of The Propulsion System." Roskam Aviation and Engineering Corporation. Kansas: Ottawa, 1989b.
30. Roskam, J. "Airplane Design: Part VI, Preliminary Calculation of Aerodynamic, Thrust and Power Characteristics." Roskam Aviation and Engineering Corporation. Kansas: Ottawa, 1989c.
31. Ruijgrok, G.J.J. "Elements of Airplane Performance." Netherlands: Delft University Press, 1990. pp. 136-157.
32. Rumelhart, D.E., Hinton, G.E., Williams, R.J., "Parallel Distributed Processing: Learning Internal Representations by Error Propagation," *Vol. 2*. Cambridge MA: The MIT Press.
33. Saltz, D., "A Short Calculus: an applied approach." California: Goodyear Publishing Co. 1974.
34. Scales, L.E., "Introduction to NON-Linear Optimization." New York: Springer-Verlag, 1985.
35. Schiff, Daniel., D'Agostino, Ralph. B., "Practical Engineering Statistics." New York, John Wiley & Sons, Inc., 1996.
36. "SIMMOD User's Manual." CACI Products Company. Arlington, VA., 1989a.
37. "SIMMOD Reference Manual." CACI Products Company. Arlington, VA., 1989b.
38. "SIMMOD Data Input Manual." CACI Products Company. Arlington, VA., 1989c.
39. United States Standard Atmosphere; 1962: Geopotential Altitude.
40. United States. House of Representatives. Committee on Science. Subcommittee on Technology. Federal Aviation Admin. Research and Organizational Management. 104 Congress, first session. May 16, 1995.

41. Vinh, Nguyen. X., "Aircraft Performance." *Cambridge Aerospace Series 4*. New York: Cambridge University Press. 1993.
42. Widrow, B., and M.E. Hoff. 1960. "Adaptive Switching Circuits." *IRE WESCON Convention Record* 4:96-104.

APPENDIX A

Aircraft Core Coefficients

% Aircraft	B747-100
% Engines	JT9D-3A
% VNE	517[knots]
% VS	110[knots]
% Idle Fuel Consumption	800[lb/hr]
% MTOW	733000[lb]
% EW	400000[lb]
% Number of Engines	4
% Wing Area	5500[ft^2]

Core Equations

.21105264	.0195524624
.263755463	-2.17159804E-03
-.16161515	8.49267355E-05
.0758395116	5500
.0249066916	4
-.0253689568	733000
.149698643	
.493944407	
.0738636868	
-.223604847	
-7.00041482E-03	
.0328436526	
.0435177226	
5.14188666E-03	
1.34403024E-03	
.0306193895	
9.83454066E-03	
-8.45369234E-03	
.0151073814	
-1.10763705E-06	
4.49822265E-08	
.0542092256	
-8.53030039E-03	
1.13895091E-03	
-6.32908055E-05	
1.28082643E-06	
-9.2774075E-04	

Aircraft Core Coefficients

% Aircraft	B767-200
% Engines	CF6-80A
% VNE	518[knots]
% VS	119[knots]
% Idle Fuel Consumption	550[lb/hr]
% MTOW	300000.[lb]
% EW	175300[lb]
% Number of Engines	2
% Wing Area	3050[ft^2]

Core Equations

.0368209248	5.88580465E-05
.369535404	1.01565402E-06
-.0794615057	1.65178004E-03
1.19172123E-03	4.11909335E-03
.0126832447	-1.58661376E-03
-9.64166545E-03	2.45352206E-04
.220878642	3050
.637665565	2
.076206901	300000
-.291661654	
-4.33010235E-03	
.0285686323	
.0332591028	
-.0818162599	
-3.73336704E-03	
.0382619471	
-1.93000345E-03	
7.39639837E-03	
200	
325	
0	
45000	
.0121599103	
2.81166465E-05	
4.38357117E-08	
.0319986281	
9.8614769E-03	
-1.71543457E-03	

Aircraft Core Coefficients

% Aircraft	DASH-7
% Engines	PT6A-50
% VNE	231[knots]
% VS	100[knots]
% Idle Fuel Consumption	150[lb/hr]
% MTOW	44000[lb]
% EW	27600[lb]
% Number of Engines	2
% Wing Area	860[ft^2]

Core Equations

.0378468694	-.0396363174
-.0397568785	1.18038287
-6.11851844E-03	1.12145574
-7.30640239E-04	-1.93252476
5.69681434E-03	.541605849
-.0181243268	860.0
-1.20089562	2.
6.02542599	44000.
-.0523632417	
-.482001873	
-.231751712	
.961104162	
7.25989187	
-35.3552068	
-1.03362163	
8.4515499	
3.20630902	
-13.0177043	
150	
230	
0	
20000	
.0357470547	
-8.4236005E-03	
8.99588121E-04	
.715305576	
-1.422529	
.703446842	
-5.36434698E-03	

Aircraft Core Coefficients

% Aircraft	DC10-30
% Engines	CF6-50A
% VNE	530[knots]
% VS	106[knots]
% Idle Fuel Consumption	550[lb/hr]
% MTOW	565000[lb]
% EW	118860[lb]
% Number of Engines	3
% Wing Area	3958[ft^2]

Core Coefficients

.0969402237	5.43086401E-06
.226048248	.0276335295
-.0360260455	-5.60263473E-03
-.0706469468	-8.20214212E-04
3.25553256E-03	1.76284875E-04
6.93085303E-03	3958.
.176102017	3.
.688138063	565000.
.0243108193	
-.124942906	
1.00018273E-03	
9.17626224E-03	
.0493856238	
-.0755815678	
6.91019055E-03	
4.82393939E-03	
-1.40794519E-03	
1.81113083E-03	
200	
300	
0	
45000	
.0155081538	
1.97064056E-05	
-3.715255E-09	
.0431748477	
2.08393033E-03	
4.49095588E-04	
-1.26675922E-04	

Aircraft Core Coefficients

% Aircraft	JETSTAR
% Engines	TFE731-3
% VNE	505[knots]
% VS	92[knots]
% Idle Fuel Consumption	100[lb/hr]
% MTOW	42000[lb]
% EW	26000[lb]
% Number of Engines	4
% Wing Area	542.5[ft^2]

Core Equations

.0134841031	1.21881272E-03
.0303350088	-4.12300952E-05
-4.51805667E-03	.639278364
-3.79565448E-03	-.246838727
3.52973105E-04	.0320710432
8.16723206E-05	-1.38999953E-03
.365299873	542.5
.656439584	4
.0266137971	42000
-.251847417	
-6.88010077E-03	
.0317623623	
.406080785	
-.867605946	
-.26626554	
.852064046	
.113603167	
-.109188801	
190	
280	
0	
45000	
.0246452545	
-2.44355304E-04	
2.74194508E-06	
-.149335028	
.0919067503	
-.0144818473	

APPENDIX B

Aircraft Fuel Consumption Model Program

```
%*****A F C M 2 7 BOEING 747-100*****

% Title      :FUEL CONSUMPTION MODEL
% Author     :Glenn D. Schilling

%FUEL BURN MODEL CORE EQUATION

% Velocity and Altitude Inputs

Vlow = 195; Vhigh = 265; Hlow = 0; Hhigh = 45000;

pts = 600;      % Number of random points
R = rand(pts,2); % Random Generator
for i=1:1:pts;

    v(i) = Vlow + (Vhigh-Vlow)*R(i,1);
    A(i) = Hlow + (Hhigh-Hlow)*R(i,2);
    h(i) = A(i)*0.0001;

    if A(i) <= 10000
        v(i) = Vlow + (250-Vlow)*R(i,1);
    elseif A(i) > 30000
        v(i) = 220 + (240-Vlow)*R(i,1);
    end

% Air Density and ICAO Standard Atmosphere

if A(i) <= 36089
    rho(i) = 0.0023769*[1-6.88*10^(-6)*(A(i))]^4.2563; % Air Density
    sv(i) = 661.5 - [(661.5 - 573.6)/36089]*A(i); % Sonic Velocity
elseif A(i) > 36089
    rho(i) = 0.00070627*exp((36089-A(i))/20806.6);
    sv(i) = 573.6;end
    sig(i) = rho(i)/0.0023769; % Atmospheric Density Ratio
    r(i) = 1/sig(i);

% Mach Number

M(i) = sqrt(5*[(r(i))*((1+0.2*[v(i)/661.5]^2)^3.5-1)+1]^0.286-1)];

RHO(i) = (1+M(i))/(1-M(i)); % Mach Number Ratio

% Velocity Calibration [ TAS, ft/sec ]

V(i) = M(i)*sv(i)*1.6867;
Vkts(i) = M(i)*sv(i);

O = max(max(Vkts));% Normalize Function

% Fuel Flow Constants

format long
fid = fopen('b747.dat');
c = fscanf(fid,'%g',[33]);
```

```

fclose(fid);
C1=c(1);C2=c(2);C3=c(3);C4=c(4);C5=c(5);C6=c(6);C7=c(7);
C8=c(8);C9=c(9);C10=c(10);C11=c(11);C12=c(12);C13=c(13);
C14=c(14);C15=c(15);C16=c(16);C17=c(17);C18=c(18);K1=c(19);
K2=c(20);K3=c(21);K4=c(22);K5=c(23);K6=c(24);K7=c(25);
K8=c(26);K9=c(27);K10=c(28);K11=c(29);K12=c(30);Sw=c(31);
N=c(32);W=c(33);

% Functions of Fuel Flow

F1(i)=C1+C2*M(i)+C3*h(i)+C4*M(i)*h(i)+C5*h(i)^2+C6*M(i)*h(i)^2;
F2(i)=[C7+C8*M(i)+C9*h(i)+C10*M(i)*h(i)+C11*h(i)^2+C12*M(i)*h(i)^2]*(N*10^4)^(-1);
F3(i)=[C13+C14*M(i)+C15*h(i)+C16*M(i)*h(i)+C17*h(i)^2+C18*M(i)*h(i)^2]*(N*10^4)^(-2);

% Functions of Mach Number

Ma(i) = K1+K2*RHO(i)^2+K3*RHO(i)^4;
Mb(i) = K4+K5*RHO(i)+K6*RHO(i)^2+K7*RHO(i)^3+K8*RHO(i)^4;
Mc(i) = K9+K10*RHO(i)+K11*RHO(i)^2+K12*RHO(i)^3;

% Total Drag Coefficient

Cd(i)=Ma(i)+Mb(i)*(W/(0.5*rho(i)*Sw*V(i)^2))^2+Mc(i)*(W/(0.5*rho(i)*Sw*V(i)^2))^4;

% Thrust Coefficient

Thrust(i) = 0.5*rho(i)*Sw*V(i)^2*Cd(i);

format short
% Fuel Flow per Engine (lb/hr)

Wf(i) = [F1(i)+F2(i)*Thrust(i)+F3(i)*Thrust(i)^2]*10000;

% Lift over Drag Ratio

Cl(i) = W/(0.5*rho(i)*Sw*V(i)^2);
LD_Ratio(i) = Cl(i)/Cd(i);

end

U = max(max(Wf));% Normalize Function

%Plot Speed vs. Velocity

subplot (1,2,1);
plot (v,A,'+');
title(' VELOCITY - ALTITUDE PROFILE');
xlabel(' Velocity IAS [knots]');
ylabel(' Altitude [ft]');
subplot (1,2,2);
plot (Vkts,A,'*');
title(' VELOCITY - ALTITUDE PROFILE');
xlabel(' Velocity TAS [knots]');
ylabel(' Altitude [ft]');
save va1747
pause
clf
plot(Vkts,Wf,'+');
title(' AFBM');
xlabel(' Velocity TAS [knots]');
ylabel(' Fuel Consumption [lb/hr]');

```

```

grid
save afbm747.ps
% *****
% Function approximation with Levenberg-Marquardt.
% Invoke the Neural Network
%     The function of the neural network learns as it passes
%     through these data points.
% *****

% Data Points (Input and Target Vectors)

P = [Vkts/O;A/45000;];% Input
T1 = Wf/U;% Target

S1 = 7;% Number of hidden neurons in the first layer

df = 10; % Frequency of progress displays (in epochs).
me = 1000; % Maximum number of epochs to train.
eg = 0.005; % Sum-squared error goal.
tp = [df me eg];

% *****
% INITFF is used to initialize the weights and biases for
% the Two Layer (TANSIG/PURELIN) network.
% *****

[w11,b11,w21,b21] = initff(P,S1,'tansig',T1,'purelin');% Initialize
% Weights and Biases

% *****
% TRAINLM - Trains a feed-forward network with faster bckprp.
% *****

% Training the Neural with a Levenberg-Marquardt Backpropagation Algorithm

[w11,b11,w21,b21,ep,tr]=trainlm(w11,b11,'tansig',w21,b21,'purelin',P,T1,tp);

save sseb747.ps
% *****
% SIMUFF - Simulates a feed-forward network.
% *****
% Trained Fuel Consumption
flops(0);
TWf= simuff(P,w11,b11,'tansig',w21,b21,'purelin')*U;
flops
X = Wf';
Y = TWf';
Z = [X Y];
plot(Vkts,Wf,'*','Vkts,TWf','+');
title('AFBM vs TRAINED FUEL CONS.');
```

```

xlabel('Velocity TAS [knots]')
ylabel('Fuel Consumption {lb/hr}')
grid
save tvsafbm747.ps
save twf747.dat Z -ascii

% *****
% USING THE PATTERN ASSOCIATOR
% *****
vlow = 195; vhigh = 265; hlow = 0; hhigh = 45000;

```

```

points = 600;% Number of random points
r = rand(points,2);% Random Generator
for i=1:1:pts;

    vel(i) = vlow + (vhigh-vlow)*r(i,1);
    alt(i) = hlow + (hhigh-hlow)*r(i,2);
    h1(i) = alt(i)*0.0001;

if alt(i) <= 10000
    vel(i) = vlow + (250-vlow)*r(i,1);
elseif alt(i) > 30000
    vel(i) = 220 + (240-vlow)*r(i,1);
end

if alt(i) <= 36089
    Rho(i) = 0.0023769*[1-6.88*10^(-6)*(alt(i))]^4.2563; % Air Density
    Sv(i) = 661.5 - [(661.5 - 573.6)/36089]*alt(i);% Sonic Velocity
elseif alt(i) > 36089
    Rho(i) = 0.00070627*exp((36089-alt(i))/20806.6);% Air Density
    Sv(i) = 573.6;% Sonic Velocity
end
Sig(i) = Rho(i)/0.0023769; % Atmospheric Density Ratio
Dr(i) = 1/Sig(i);

% Mach Number

Mn(i)=sqrt(5*[(Dr(i)*((1+0.2*[vel(i)/661.5]^2)^3.5-1)+1)^0.286-1]);

mnr(i) = (1+Mn(i))/(1-Mn(i)); %Mach Number Ratio

% Sonic Velocity [ TAS, ft/sec ]

Vfs(i) = Mn(i)*Sv(i)*1.6867;
Vknobs(i) = Mn(i)*Sv(i);

% *****
% Neural Generalized Data can be Implemented back to
% the Original Base Fuel Consumption Algorithm
% to test the accuracy of Neural Nets Generalization
% and to see if the inputs (Velocity and Altitude)and
% targets fit within a marginal error.
% *****

% Functions of Fuel Flow

F11(i)=C1+C2*Mn(i)+C3*h1(i)+C4*Mn(i)*h1(i)+C5*h1(i)^2+C6*Mn(i)*h1(i)^2;
F21(i)=[C7+C8*Mn(i)+C9*h1(i)+C10*Mn(i)*h1(i)+C11*h1(i)^2+C12*Mn(i)*h1(i)^2]*(N*10^4)^
(-1);
F31(i)=[C13+C14*Mn(i)+C15*h1(i)+C16*Mn(i)*h1(i)+C17*h1(i)^2+C18*Mn(i)*h1(i)^2]*(N*10
^4)^(-2);

% Functions of Mach Number

Ma1(i) = K1+K2*mnr(i)^2+K3*mnr(i)^4;
Mb1(i) = K4+K5*mnr(i)+K6*mnr(i)^2+K7*mnr(i)^3+K8*mnr(i)^4;
Mc1(i) = K9+K10*mnr(i)+K11*mnr(i)^2+K12*mnr(i)^3;

% Total Drag Coefficient

Cd1(i)=Ma1(i)+Mb1(i)*(W/(0.5*Rho(i)*Sw*Vfs(i)^2))^2+Mc1(i)*(W/(0.5*Rho(i)*Sw*Vfs(i)^2)
^4;

```

```

% Thrust Coefficient (lb)

Thrust1(i) = 0.5*Rho(i)*Sw*Vfs(i)^2*Cd1(i);

% Fuel Flow per Engine (lb/hr)

BWf(i) = [F11(i)+F21(i)*Thrust1(i)+F31(i)*Thrust1(i)^2]*10000;

end

Q = max(max(Vknots));% Normalize Function

%*****
% Generalization
% We can now test the associator with different random
% inputs, and see if it returns the target.
%*****

p = [Vknots/Q;alt/45000;];

% Generalized Fuel Consumption

GWf = simuff(p,w11,b11,'tansig',w21,b21,'purelin')*U;

y = GWf';
x = BWf';
z = [y x];
save cmpb747.dat y x -ascii;

%*****
subplot(2,1,1);
plot(M,Cd,'*');
title('Lift over Drag');
xlabel('Mach #');
ylabel('Drag Coeff. ');
grid;
subplot(2,1,2);
plot(M,LD_Ratio,'*');
title('Lift over Drag');
xlabel('Mach #');
ylabel('Lift/Drag');
grid;
save ldb747.ps
pause
clf
subplot(3,1,1)
plot(M,Ma,'*');
title('Lift over Drag');
xlabel('Mach #');
ylabel('Ma');
grid;
subplot(3,1,2);
plot(M,Mb,'*');
title('Lift over Drag');
xlabel('Mach #');
ylabel('Mb');
grid;
subplot(3,1,3);
plot(M,Mc,'*');
title('Lift over Drag');
xlabel('Mach #');

```

```

ylabel('Mc');
grid;
save MvsMib747.ps
pause
clf
subplot(3,1,1);
plot( Vknots,GWf,'*');
title('GENERALIZED FUEL CONSUMPTION');
xlabel('Velocity TAS [knots]');
ylabel('Fuel Consumption [lb/hr]');
grid;
subplot(3,1,2);
plot3( Vknots,alt,GWf,'*');
title('GENERALIZED FUEL CONSUMPTION');
xlabel('Velocity TAS [knots]');
ylabel('Altitude [ft]');
zlabel('Fuel Consumption [lb/hr]');
grid;
subplot(3,1,3);
plot(Vkts,TWf,'*',Vknots,GWf,'+');
title('TRAINED Wf vs. GENERALIZED Wf');
xlabel('Velocity');
ylabel('Fuel Consumption');
grid;
save subwfb747.ps
pause
clf
plot(Vknots,GWf,'+',Vknots,BWf,'*');
title('GENERALIZED Wf vs GENERALIZED AFBM');
xlabel('Velocity');
ylabel('Fuel Consumption');
grid
save gbb747.ps

%*****STATISTICS*****

%difference of general and general AFBM = x - y
%The sum of the difference is divided by the sample size
%      sw = sum(w)/600 = mean(w)
% CALCULATING THE MEANS
% x = GENERALIZED DATA
% y = AFBM AFTER INVOKING THE NEURAL NET GENERALIZED DATA
w = y - x;
save sd747.dat y x -ascii
m = mean(w);
% W = THE DIFFERENCE OF THE SAMPLE MEANS
% CALCULATING THE RMS (Standard Deviation)
s1 = (sum(w.^2)-(sum(w)^2/600))/599;
% CALCULATING THE PAIRED SAMPLE t-TEST
t = m/(sqrt(s1/600))
hist(w)

```

Specific Input Variable Program for the Aircraft Fuel Consumption Model

```
%*****A F C M 2 7 BOEING 747-100*****

Vkts =                240;
A =                  25000;

P = [Vkts/O;A/45000;];% Input

flops(0);
TWf= simuff(P,w11,b11,'tansig',w21,b21,'purelin')*U
flops*600

Vknots =              240;
alt =                  25000;

p = [Vknots/Q;alt/45000;];

flops(0);
GWf = simuff(p,w11,b11,'tansig',w21,b21,'purelin')*U

flops*600

pause
clf
subplot(1,2,1)
plot(Vknots,GWf,'b*');
xlabel('Velocity TAS [knots]')
ylabel('Fuel Consumption [lb/hr]');
grid;
subplot(1,2,2)
plot(Vkts,TWf,'m+');
xlabel('Velocity TAS [knots]');
ylabel('Fuel Consumption [lb/hr]');
grid;
print -depsc comp747.eps
```

APPENDIX C

T-Test of the Mean for the Trained Data

T-Test of the Mean

Test of $\mu = 0.00$ vs $\mu \text{ not } = 0.00$

Variable	N	Mean	StDev	SE Mean	T	P-Value
747-100	600	3.97	77.76	3.18	1.25	0.21

MTB > ttest 0 c3

T-Test of the Mean

Test of $\mu = 0.000$ vs $\mu \text{ not } = 0.000$

Variable	N	Mean	StDev	SE Mean	T	P-Value
767-200	600	0.611	22.200	0.907	0.67	0.50

MTB > ttest 0 c3

T-Test of the Mean

Test of $\mu = 0.0000$ vs $\mu \text{ not } = 0.0000$

Variable	N	Mean	StDev	SE Mean	T	P-Value
Dash-7	600	0.0117	1.6870	0.0689	0.17	0.87

MTB > ttest 0 c3

T-Test of the Mean

Test of $\mu = 0.00$ vs $\mu \text{ not } = 0.00$

Variable	N	Mean	StDev	SE Mean	T	P-Value
DC-10	600	2.23	34.10	1.39	1.60	0.11

MTB > ttest 0 c3

T-Test of the Mean

Test of $\mu = 0.000$ vs $\mu \text{ not } = 0.000$

Variable	N	Mean	StDev	SE Mean	T	P-Value
Jetstar	600	-0.014	3.155	0.129	-0.11	0.91

T-Test of the Mean and Confidence Level for the Generalized Data

T-Test of the Mean

Test of mu = 0.00 vs mu not = 0.00

Variable	N	Mean	StDev	SE Mean	T	P-Value
747-100	600	23.97	76.25	3.11	7.70	0.0000

MTB > tinterval 99 c3

Confidence Intervals

Variable	N	Mean	StDev	SE Mean	99.0 % C.I.
747-100	600	23.97	76.25	3.11	(15.93, 32.02)

MTB > ttest 0 c1

T-Test of the Mean

Test of mu = 0.00 vs mu not = 0.00

Variable	N	Mean	StDev	SE Mean	T	P-Value
767-200	600	0.95	37.79	1.54	0.62	0.54

MTB > tinterval 99 c1

Confidence Intervals

Variable	N	Mean	StDev	SE Mean	99.0 % C.I.
767-200	600	0.95	37.79	1.54	(-3.03, 4.94)

T-Test of the Mean

Test of mu = 0.00 vs mu not = 0.00

Variable	N	Mean	StDev	SE Mean	T	P-Value
Dash-7	600	1.36	1.46	0.06	22.8	0.0000

MTB > tinterval 99 c1

Confidence Intervals

Variable	N	Mean	StDev	SE Mean	99.0 % C.I.
Dash-7	600	1.36	1.46	0.06	(1.2, 1.5)

T-Test of the Mean and Confidence Level for the Generalized Data

T-Test of the Mean

Test of $\mu = 0.00$ vs $\mu \text{ not } = 0.00$

Variable	N	Mean	StDev	SE Mean	T	P-Value
DC10-30	600	32.80	58.70	2.40	13.71	0.0000

MTB > tinterval 99 c1

Confidence Intervals

Variable	N	Mean	StDev	SE Mean	99.0 % C.I.
DC10-30	600	32.80	58.70	2.40	(26.7, 39.1)

T-Test of the Mean

Test of $\mu = 0.00$ vs $\mu \text{ not } = 0.00$

Variable	N	Mean	StDev	SE Mean	T	P-Value
Jetstar	600	2.05	5.72	0.23	8.8	0.0000

MTB > tinterval 99 c1

Confidence Intervals

Variable	N	Mean	StDev	SE Mean	99.0 % C.I.
Jetstar	600	2.05	5.72	0.23	(1.45, 2.65)

APPENDIX D

Boeing 747-100

Final Weights and Bias of First Layer (tansig transfer function)

w11 =

4.3300 -5.0906
2.8216 1.9130
-7.1883 2.9530
3.5891 4.7336
4.0930 0.4112
-2.3440 -2.7255
-4.5788 2.7907

b11 =

2.2097
-2.9428
1.1362
-6.6396
-3.4117
2.9470
6.0262

Final Weights and Bias of Second Layer (purelin transfer function)

w21 =

-2.9916 -0.8265 1.4365 -0.0504 0.3530 -0.5334 0.2561

b21 =

4.4166

Boeing 767-200

Final Weights and Bias of First Layer (tansig transfer function)

w11 =

5.9433 1.6654
3.0375 0.2118
4.9063 -0.9624
-2.1943 -3.4444
0.5762 3.3591
-5.3369 -0.5420
-0.7713 -2.3823

b11 =

-7.3605
-2.8671
-3.3723
6.2683
-1.8215
6.3248
2.7198

Final Weights and Bias of Second Layer (purelin transfer function)

w21 =

-1.7628 -1.4865 0.6767 -2.0824 0.0558 -3.8428 -0.3741

b21 =

4.2202

Bombardier Dash-7

Final Weights and Bias of First Layer (tansig transfer function)

w11 =

1.8984 -0.1980
-5.5588 0.9014
3.8653 0.6499
2.4640 0.5639
9.5165 0.3771
-0.7353 1.2700
-0.5016 -0.7420

b11 =

-2.0500
4.0909
-2.7994
-1.8912
-9.6398
-0.2296
0.7715

Final Weights and Bias of Second Layer (purelin transfer function)

w21 =

-18.4723 -1.2817 -6.4901 20.4800 2.0058 2.8261 16.9011

b21 =

-10.4035

McDonnell-Douglas DC10-30

Final Weights and Bias of First Layer (tansig transfer function)

w11 =

2.8067 -2.3443
2.3617 0.1115
-4.2343 -2.0659
-7.9688 2.6974
-4.8719 1.4929
0.2293 -0.3729
2.6228 -0.3914

b11 =

-1.8534
-2.1917
7.9116
4.0465
3.5858
-4.2763
-2.2856

Final Weights and Bias of Second Layer (purelin transfer function)

w21 =

-0.6066 6.4040 -10.4683 -0.5452 -5.0632 -3.5148 -15.7285

b21 =

4.5926

Lockheed Martin Jetstar

Final Weights and Bias of First Layer (tansig transfer function)

w11 =

-5.1453 4.6796
-4.6448 -1.9562
1.5857 -0.4753
1.5416 1.2068
1.3869 -0.0271
10.4969 -2.9506
-6.5130 4.9539

b11 =

2.4444
6.8439
-4.4989
-3.9635
-0.0464
-4.0000
-1.1425

Final Weights and Bias of Second Layer (purelin transfer function)

w21 =

-0.1229 -0.4898 -0.9497 -2.2306 0.9549 -0.6043 5.0197

b21 =

2.9107

VITA

Glenn Douglas Schilling was born in Northport, New York, on September 4, 1969. In May 1992 he graduated from Rochester Institute of Technology (RIT), New York, with a Bachelor of Science in Civil Engineering. While pursuing his bachelor's degree at RIT he was involved with the cooperative education plan (co-op), where he incorporated one year of work experience into his education. After working two years at a consulting firm in Long Island New York, he came to Virginia Polytechnic Institute and State University, Virginia, in the spring of 1994 to pursue his graduate studies. In the spring of 1997 he completed his degree of Master of Science in Civil Engineering, specializing in Transportation Engineering.

Mr. Schilling plans on starting his career in the transportation engineering arena upon graduation at Virginia Polytechnic Institute and State University, Virginia.